

Review

# Green Derived Zinc Oxide (ZnO) for the Degradation of Dyes from Wastewater and Their Antimicrobial Activity: A Review

Louisah M. Mahlaule-Glory  and Nomso C. Hintsho-Mbita \* 

Department of Chemistry, DSI/NRF Centre of Excellence in Strong Materials, University of Limpopo, Sovenga, Polokwane 0727, South Africa; louisah.mahlauleglory@ul.ac.za

\* Correspondence: nomso.hintsho-mbita@ul.ac.za; Tel.: +27-(0)-15-268-2205

**Abstract:** The quest for eco-friendly synthetic routes that can be used for the development of multifunctional materials, in particular for water treatment, has reinforced the use of plant extracts as replacement solvents in their use as reducing and capping agents during the synthesis of green derived materials. Amongst the various nanoparticles, Zinc Oxide (ZnO) has emerged as one of the preferred candidates for photocatalysis due to its optical properties. Moreover, ZnO has also been reported to possess antimicrobial properties against various bacterial strains such as *E. coli* and *S. aureus*. In this review, various types of pollutants including organic dyes and natural pollutants are discussed. The treatment methods that are used to purify wastewater with their limitations are highlighted. The distinguishing properties of ZnO are clearly outlined and defined, not to mention the performance of ZnO as a green derived photocatalyst and an antimicrobial agent, as well. Lastly, an overview is given of the challenges and possible further perspectives.

**Keywords:** ZnO; organic dyes; photocatalytic activity; antimicrobial analysis



**Citation:** Mahlaule-Glory, L.M.; Hintsho-Mbita, N.C. Green Derived Zinc Oxide (ZnO) for the Degradation of Dyes from Wastewater and Their Antimicrobial Activity: A Review. *Catalysts* **2022**, *12*, 833. <https://doi.org/10.3390/catal12080833>

Academic Editor: Ioannis Konstantinou

Received: 1 July 2022

Accepted: 26 July 2022

Published: 29 July 2022

**Publisher's Note:** MDPI stays neutral with regard to jurisdictional claims in published maps and institutional affiliations.



**Copyright:** © 2022 by the authors. Licensee MDPI, Basel, Switzerland. This article is an open access article distributed under the terms and conditions of the Creative Commons Attribution (CC BY) license (<https://creativecommons.org/licenses/by/4.0/>).

## 1. Introduction

Water is a required element and nutrient servicing humans, plants and animals. Various factors such as lack of rainfall, water pollution, climate change, economic growth, poor water management and population growth have led to a shortage of water [1]. South Africa is regarded as one of the 36 water-scarce countries (Figure 1).

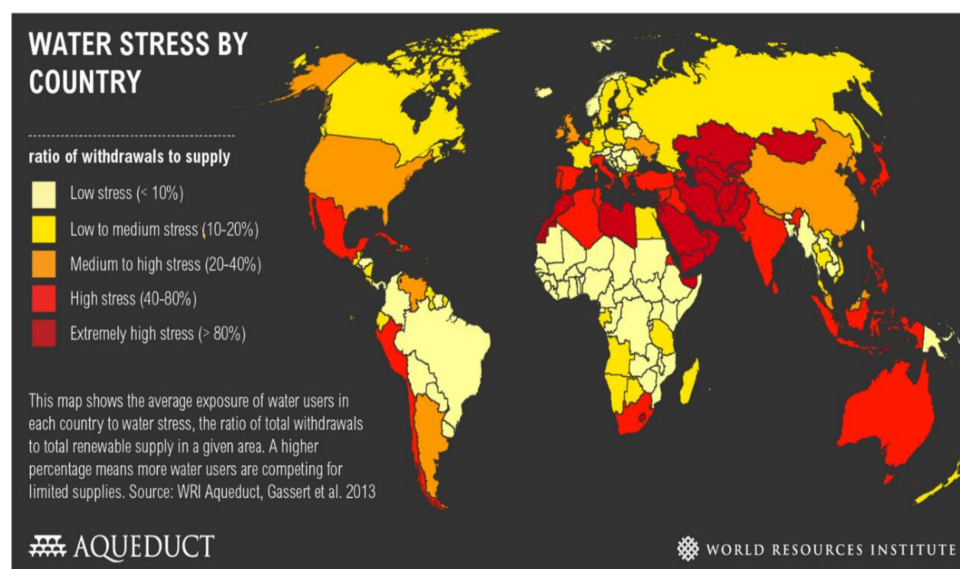


**Figure 1.** Global overview of water shortage [2].

One of the major factors that generates water crisis in several parts of the world and contributes to wastewater is water pollution. Through various reports, it has been discovered that organic dyes are the major contributors to wastewater, followed by pharmaceutical pollutants, leaving natural pollutants as the least benefactor towards wastewater [3,4]. A summarised version of these pollutants is displayed on a schematic diagram in Figure 2 [5–7].

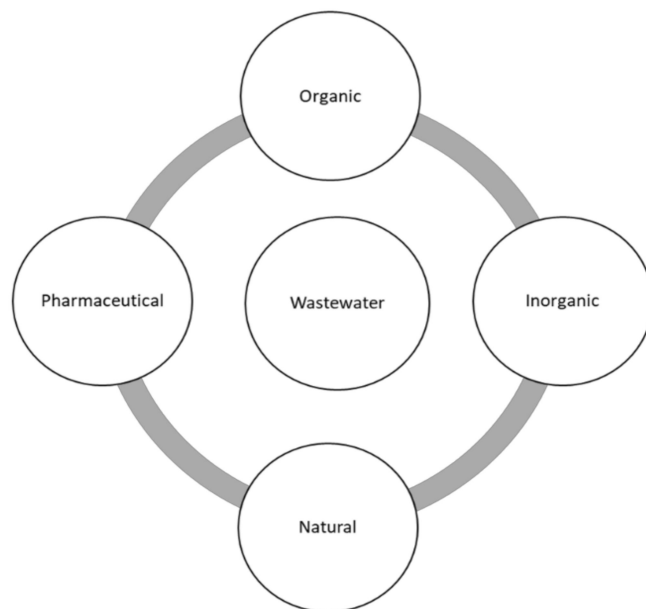


**Figure 2.** Schematic illustration of various pollutants in wastewater pollution.

Organic dyes remain a global environmental controversy and this is due to the manner in which they are inaccurately discharged into the wastewater. It is estimated that about 80% of wastewater is discharged without treatment to different water streams [4]. Researchers, therefore, reported that the majority of wastewater constituent is organic dyes. Over and above, Ayele et al. [8] further estimated that between 10–15% of discharged wastewater is contributed by organic dyes [8,9].

Dyes are essentially used for colouring or colour changing especially in materials such as food, cosmetics, furniture, clothes, wool, leather, paper, rubber and many others [10–12]. Colour compounds (dyes) can be made from natural compounds or synthetic (human-made) methods. Natural colour compounds can be extracted from phytochemicals from vegetables and animals, respectively. These include anthraquinones (red), flavonoids (yellow) and indigoids (blue and violet) [13]. However, synthetic dyes are water-soluble, aromatic and dispersible organic colourants utilised within the environment [8] dispersed from industries such as textile, printing, tannery, pharmaceuticals, food cosmetics and many more [14–16]. Textile industries appear to be the largest consumer of synthetic dyes in consequences of cost-effectiveness, ease of use, higher light stability and firmness against temperature, microbes, detergents and colour variety as compared to natural dyes [17]. Therefore, it has been reported to cause life-threatening illnesses like brain damage, kidney failure, cancer and skin irritation after consumption [5,18]. Our focus on the organic dyes will be reporting mainly on the Methylene Blue (MB) dye from this review.

Other pollutants that have been of interest lately are bacterial strains such as *Escherichia coli* (*E. coli*), *Enterobacter faecalis* (*E. faecallis*), *Staphylococcus aureus* (*S. aurea*) and *Pseudomonas aeruginosa* (*P. aeruginosa*). These natural pollutants originate from the hospital and industrial effluents, which include human faeces floating and creating sewage water [19]. Not to mention that they are captured, accumulated, replicated and continue to spread into pathogens through wastewater if not treated in time [20]. This causes these strains to be highly toxic, pathogenic and hazardous, which poses a serious health threat to the ecosystem and the environment [21]. When these pollutants are above the permissible levels, they

tend to cause all kinds of illnesses such as septicaemia, destructive lesions, bacteraemia, fibrosis, immunocompromised pulmonary infection, renal failure, urinary tract infections, meningitis and many more [22,23]. What is more is that other water bodies including lakes, pools and rivers have also attracted natural pollutants like hotspots [4,24,25]. In addition to that, the rainfall-runoff tends to also be conveyed and concentrated while they generate themselves into natural pollutants moving towards water streams [4].

Researchers are currently working towards the development of sustainable methods that can be used to combat water pollution and poor water management. Amongst the documented treatment strategies, Advanced Oxidation Processes (AOP) is a well-studied treatment method that has been used to treat organic dyes since they are biodegradable. This method uses the oxidation-reduction process, which produces hydroxyl radicals, which are powerful oxidants in the presence of the materials used to degrade complex organic structures such as organic dyes [26]. Methods such as ozone, Fenton's reagent, electrocoagulation and photocatalysis are some of the AOPs used [18]. Ozone and electrocoagulation have been used for the saline environment and biological methods that are inactive towards textile wastewater since the organic dyes cannot degrade them biologically [27]. However, amongst these AOP methods, photocatalysis is the method of choice as it can degrade dyes and various other pollutants by the generation of hydroxyl radicals in an inert environment [28]. In addition, they do not produce secondary pollutants like hydrogen peroxide ( $H_2O_2$ ) as has been noted from the Fentons reagent method [29].

Nanotechnology is an upcoming field that researchers are using as a tool to address health-related challenges facing our environment [28]. Nanoparticles have been identified as possible viable materials due to their multifunctional properties. The synthesis of metal oxide nanoparticles coupled with plant extracts has recently gained momentum [30,31]. These materials have properties that assist in degrading organic pollutants and inhibit pathogenic microbial strains in wastewater.

Researchers are currently moving away from general synthesis methods, which involve the use of hazardous reagents and toxic chemicals and are looking for better strategies that will mitigate these challenges [32,33]. The need for environmentally friendly materials that can be used in various applications such as photocatalysis and biomedical applications has become a priority, hence the synthesis of these materials using green chemistry. A green synthesis route is an upcoming approach that uses natural reductants such as bacteria, enzymes and plant extracts [34]. Amongst the natural reductants, plants are preferred since they are less toxic, especially when treating microorganisms and are readily available [35]. They possess various phytochemicals that are normally present in these extracts from the primary (*polyphenols* compounds, nitrogen compounds and vitamins) to secondary metabolites (*flavonols*, *amines* and *alkaloids* and *glycosides*) [36–38]. In other instances, these phytochemicals act as capping and stabilizing agents where they inhibit bacterial growth, reduce agglomeration and enhance the antimicrobial properties of metal oxide nanoparticles [39].

Amongst the well-studied materials of metal oxides, ZnO is one of the most preferred materials that possess these desired traits [17,40,41]. Compared to other materials such as  $TiO_2$ , bimetallic  $SnO_2$ - $SrO$  etc. [27,33], which have very high photocatalytic efficiencies, especially against organic dyes, this material has also been shown to have low toxicity and more stability. Moreover, ZnO is also biocompatible which means it is a better candidate for multifunctional activities. In this review, the various pollutants (dyes and bacteria) found in wastewater, their nature and origins, as well as the general treatment strategies and their limitations are discussed. The focus will also be on the properties of ZnO and their use as photocatalysts and as antimicrobial agents. We describe the challenges facing single metal oxide synthesis and lastly, we highlight the future perspectives.

## 2. Pollutants

Pollutants are a major environmental concern posing a serious health threat to the ecosystem. Organic (dyes), natural (pathogenic strains) and inorganic (heavy metals)

pollutants are generated from human activities (wastewater) such as domestic, industrial, agricultural, textile and mining effluents [42]. Additionally, poor sewage treatment, marine dumping difficulties, radioactive waste material and other agricultural activities have also contributed to the water being contaminated with various pollutants [43]. The World Health Organisation (WHO) reported that water contamination caused more than 1.7 billion deaths worldwide, hence there is a need to discuss these pollutants.

### 2.1. Organic Pollutants

Synthetic dyes are aromatic organic compounds grouped according to their ionic charge molecules like cationic, anionic and non-ionic compounds. Moreover, they can also be classified based on their colour, chemical structure, application and their particle size in a solution [44]. The chromophoric and auxochromic structures of dyes play a vital role in the identification of a dye since the chromophores are responsible for controlling dye colour by absorbing light and reflecting it into the human eye at a particular angle [8]. Whereas, the auxochromes are a group of atoms attached to the chromophore and are therefore responsible for enabling the chromophores to absorb light [8]. Based on their chemical structures, dyes can further be grouped into a variety of chromophores. A list of over 100 chromophoric groups of dyes has been reported and to name a few are the azo (mono-azo, di-azo, tri-azo and poly-azo), quinones (anthraquinone, alizarin and many others), ketones (aminoketone, hydroxyl ketone, diarylmethane and triarylmethane) phthalocyanine, indigo, indophenol, indamine, oxazine, azine, xanthene, lactone, -nitro, nitroso and methane [13,17,45,46]. Figure 3 displays some of the major chromophoric dye structures. Table 1 further indicates the different types of dyes with their chromophotic structure, ionic strengths and many more.

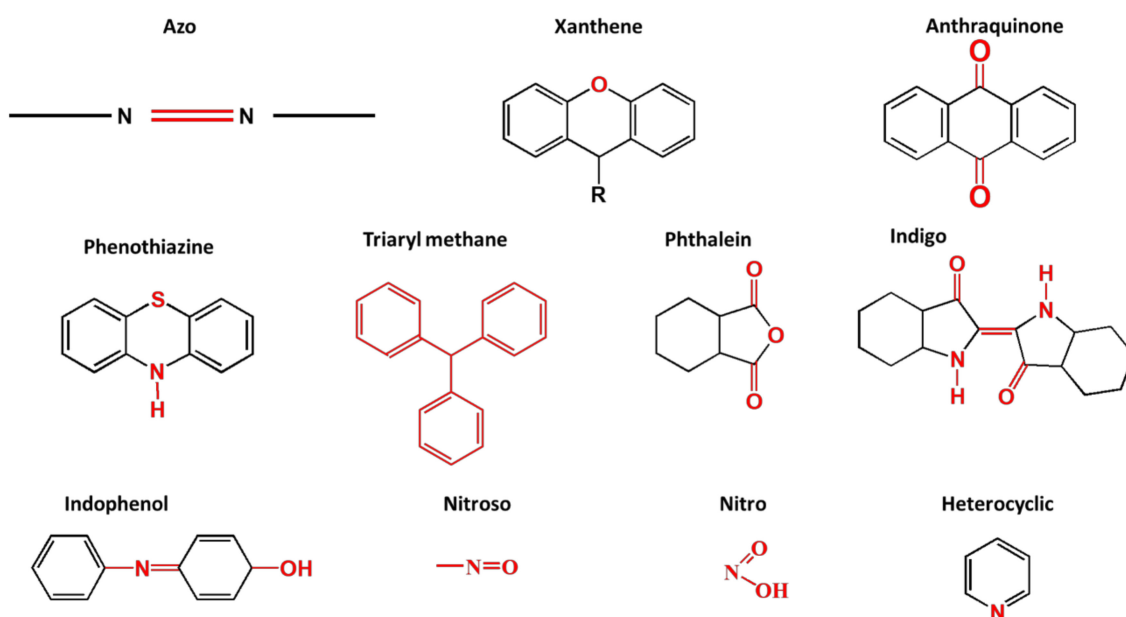


Figure 3. Chromophotic structures of the main synthetic groups in organic dyes.

**Table 1.** Various types of dyes with their chromophotic nature.

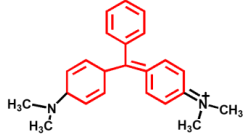
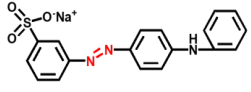
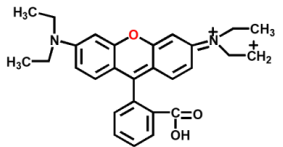
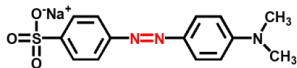
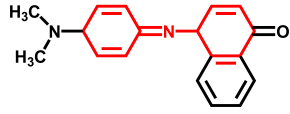
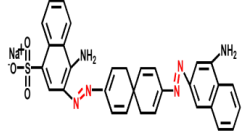
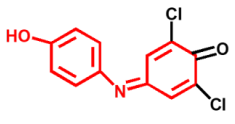
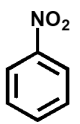
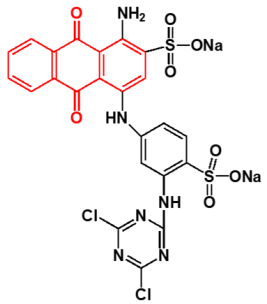
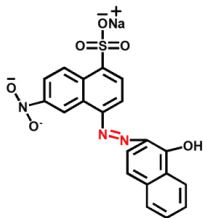
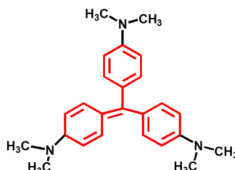
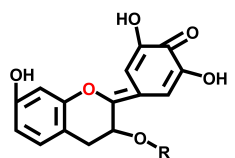
Structure	Dye Name	Chromophore	Source, Properties and Toxicity	Uses	Ref
	MB	Phenothiazine	Synthetic dye Biological properties such as antioxidant, antimalarial, antidepressant and cardioprotective properties Carcinogenic and mutagenic	Wood, leather, plastic and silk	[47–49]
	MG	Triaryl methane	Natural dye From minerals and used for mineral pigmentation Used as an antimicrobial agent for aquaculture	Food, aquaculture, textile and dyeing Silk, leather paper	[44,49–52]
	AY	Azo	Wool, silk, nylon, fabrics	Textile, paints, leather and cosmetics	[53,54]
	RHB	Xanthene	Synthetic, wastewater, tracer and fluorescence nature	Printing, paper, paints, leather, food and plastic	[55,56]
	MO	Azo	Synthetic and has sensing properties	Titration indicator, textile printing, food	[57–60]
	IB	Indophenol	Synthetic Detecting ammonia	Detection and dyeing	[61]
	CR	Azo	Synthetic Dyeing Very harmful (Carcinogenic)	Printing, cotton wool, textile, clothing, food and cosmetics	[62]
	DCPIP	Indophenol	Both naturally and synthetic Naturally from fruits and vegetables They also possess biological properties Detection of ammonia (NH <sub>3</sub> )	Titration and dyeing	[63–67]
	NB	Nitro	Synthetic Dyeing Toxic and mutagenic B <sub>2</sub> Carcinogen	Form aniline, and pesticides, used in pharmaceutical industries, manufacture explosives and also used for dyeing	[68]
	RD4	Anthraquinones	Synthetic	Cosmetics, food, paper, pharmaceutical and leather	[69,70]

Table 1. Cont.

Structure	Dye Name	Chromophore	Source, Properties and Toxicity	Uses	Ref
	EBT	Azo	Synthetic Hazardous and carcinogenic	Dyeing multifibers, wool, nylon, silk Titration indicator Formation of coloured complexes	[61,71,72]
	CV	Triarylmethane	Synthetic High thermal, reduced scattering and intrinsic polarization Difficult to crystallise Carcinogenic	Medicinal—Active ingredient in gram staining and antibacterial agent Textile—sensitiser for photoconductivity Laboratory—pH indicator, disinfectant in humans and animals	[44,61,73,74]
	A	Anthraquinones	Natural from fruits and vegetables (red cabbage, grapes, berries and many more) it has biological properties such as anticancer, anti-inflammatory, antimicrobial, antiobesity Sensitive to light, pH, heat and oxygen	Titration Indicator	[75,76]
	I	Indigo	Natural and synthetic Naturally—has biological properties like antiseptic but toxic if ingested in large volumes. Synthetic—Carcinogenic	Formulate artifacts like paintings, Chinese temple decorations, mummy clothes, Japanese woodblocks and dyeing	[77]

MB = Methylene Blue; MG = Malachite Green; MR = Methylene Red; MO = Methylene Orange; AY = Acid Yellow; RhB = Rhodamine Blue; IB = Indophenol Blue; CR = Congo Red; EBT = Eriochrome Black; CV = Crystal violet; A = Anthocyanin; I = Indigotin; NB = Nitrobenzene.

From Figure 3, it can be noted that the chromophoric structures of each dye play an essential role in the identification of that particular dye. For example, azo dyes have a double bond conjugated between the electron system connected to two nitrogen atoms as displayed and highlighted in red in Figure 3 and Table 1. Further examples of azo dyes displayed in Table 1 are acid yellow, methyl orange, congo red and Eriochrome Black, represented by the connection of the double bond between the nitrogen. This is not the same case with methylene blue as other researchers have previously reported that MB is an azo dye. However, according to its chromophoric structure from Table 1, we can simply say that it is the phenothiazine group that is observed by the nitrogen atom attached to the aryl groups rather than the missing double bond, as it is supposed to have been between the nitrogen atoms, similar to the rest of the chromophoric structures of these dyes exhibited in Table 1. Another example will be the triarylmethane which is conjugated by the three aromatic benzene structures/rings; examples include malachite green and crystal violet dye. The natural pollutants are further discussed in Section 2.2.

## 2.2. Natural Pollutants

Microorganisms are found everywhere within the aquatic world and the environment; examples include enzymes, fungi and bacteria, which can either influence by boosting or by damaging the immune system within the human body [47]. Some hazardous

and pathogenic microbial strains that have been found in the water streams include, *Escherichia coli* (*E. coli*) 28922 ATCC [MTCC 1586], *Enterobacter faecalis* (*E. faecalis*) 29212 ATCC [MTCC 439], *Staphylococcus aureus* (*S. aureus*) 43300 ATCC [MTCC 740] and *Pseudomonas aeruginosa* (*P. aeruginosa*) 287,853 ATCC [MTCC 741] [23]. According to the South African Water Quality Guidelines (SAWQG) published in 1997 and the World Health Organization (WHO), they reported that the colony-forming unit (CFU) of all the listed pathogenic strains (*E. coli*, *P. aeruginosa* and *E. faecalis*) must not exceed 0 CFU/100 mL, meaning that they should not be detectable in drinking water. However, *S. aureus* is permissible but should not exceed 110 CFU/100 mL in drinking water. If it exceeds the acceptable levels it can be toxic. Additionally, it can be transmitted through skin contact and via food contamination.

Two of the most common strains in water are *E. coli* and *P. aeruginosa*. They are both coliforms but are classified according to their cell walls, generic makeup and their shapes (Figure 4).

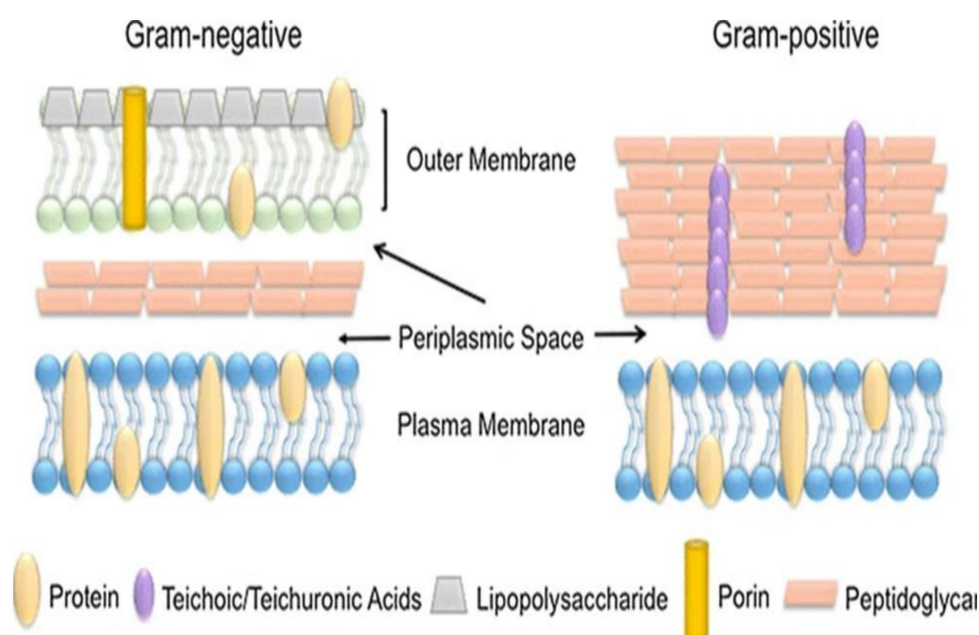


**Figure 4.** Schematic differentiation of the gram-negative and positive cells [78,79].

They can either be gram-negative or gram-positive, based on their cell wall composition. These pathogenic strains are from warm-blooded animals, and human faeces are used as indicators. If detected in drinking water, these will then indicate water contamination. The gram-positive strains (*S. aureus* and *E. faecalis*) are found in soil, pools and rivers and can be transmitted through human skin by coming in contact with water [79,80].

*E. coli* is a gram-negative strain with a rod structure which contains spores with large colonies, as indicated in Figure 5. This strain can survive in water for more than three days and replicate itself continuously if the optimum conditions are met, resulting in severe diseases. When humans are exposed to this strain, it can cause illnesses from acute haemolytic-uraemic syndrome, diarrhoea, gastroenteritis and septicemia to chronic diseases such as renal failure, urinary tract infections and meningitis [23].

*S. aureus* is a gram-positive strain that is resistant to methicillin [81]. It has a grapelike structure with a spherical base within and is found within the human skin and mucous membranes of the animals as indicated in Figure 2. It can cause gastrointestinal diseases since it is found in sewage water. When exposed to water it can multiply itself in a tissue or produce toxins in the enzymes such as endocarditis, osteomyelitis, septicemia and pneumonia [25]. If consumed in food, it can lead to severe illnesses, hence the concentration should not exceed 3 CFU/mg/mL in food [20].

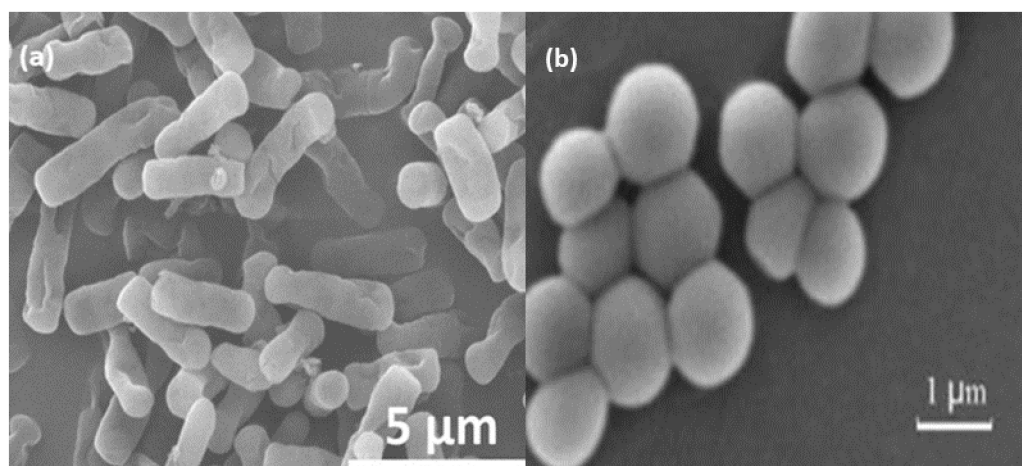


**Figure 5.** The morphological structure of (a) *E. coli* and (b) *S. aureus* [82].

### 3. Treatment Methods Used to Purify Wastewater

The pollutants in wastewater have been treated with various purification methods, namely, the reverse osmosis, adsorption, precipitation, ion exchange and biological methods, as well as coagulation and electrocoagulation [83]. However, these methods have been shown to have some limitations which are listed in Table 2.

**Table 2.** List of advantages and disadvantages of wastewater treatment methods.

Type of Method	Advantage	Disadvantage	References
Reverse Osmosis	Higher desalination High water permeability Development of thin film composite membranes	Tedious process Generate different environmental impact Energy-intensive Membrane Fouling High maintenance and operational cost	[84]
Adsorption	Simple in process design Regenerative process	Disposal of used adsorbent Difficult in regenerating used adsorbent Desorption Adsorbents tend to exhibit low adsorption capacity from adsorbents Displays slow reaction Expensive	[85,86]
Ion exchange	Use of resin or adsorbents Easily resin regeneration Rapid, efficient and effective process Suitable resins for selective pollutants	Require pre-treatment methods Capacitive deionisation Ionic competition Sensitive to pH Complex operation Fouling matrix	[87]
Biological	Natural process Eco friendly Less costly	Challenge in degrading non-biological materials	[88]
Flocculation	Biodegradable Preferred for removing fine particles Removes colour, metals and turbidity	Generation of high-volume sludge Difficulty in handling sludge Toxic if improperly used Require multiple processes High operational and disposal cost	[89,90]
AOP	Complete degradation of pollutants Involves strong oxidising agents Eco-friendly Less costly	Slow process	[10]

Table 2 displays different types of wastewater treatment methods and their advantages and disadvantages. In summary, most of these methods are shown to be expensive, generate secondary pollutants and many others. For example, reverse osmosis suffers from

membrane fouling and having high operation costs. Another method like ion exchange may require pre-treatment of the materials and could be sensitive to pH as well. Flocculation may produce large volumes of sludge, which leads to difficulty in handling it and thus results in high operational costs. Methods such as photocatalysis under the Advanced Oxidation Process (AOP) have been identified as some of the methods that have the ability to degrade a particular group of pollutants of interest such as dyes without generating secondary pollutants and offer more advantages compared to the previously mentioned methods.

### 3.1. Advance Oxidation Process (AOP)

Advance Oxidation Processes (AOP) are methods that use highly reactive species like radicals with the help of Ozone ( $O_3$ ) in the ozonation process, Fenton's reagent (Fenton process) and hydrogen peroxide ( $H_2O_2$ ) under electrochemical oxidation [91]. These methods have been reported to be effective in treating wastewater. However, they provide the frequent presence of radicals that are only selective to organic pollutants with low biodegradability, and the ozonation method works best in a saline environment [6]. On the other hand, photocatalysis is a promising method under AOP methods which has been shown to decompose organic dyes using strong oxidants such as  $OH^-$  radicals [28]. Since these other methods have the ability to produce secondary pollutants, photocatalysis has been the method of choice for many researchers as it can completely degrade dyes without producing secondary pollutants.

#### Photocatalysis

Photocatalysis is a process used to treat water by degrading pollutants, especially organic dyes, under light containing UV rays to form environmentally-friendly by-products. This process can decompose dyes like methylene blue (MB) into water ( $H_2O$ ), carbon dioxide ( $CO_2$ ) and minerals without generating secondary pollutants [6]. In addition, it is preferred due to its ability to degrade a variety of organic pollutants. The method provides rapid degradation rates, is less costly and operates under ambient conditions. Moreover, it operates in three mechanisms, namely, hydrogen abstraction, electron transfer and radical addition [92]. How photocatalysis occurs has been reported as when the light emits on the surface of the catalyst, the electrons from the valence band (VB) get excited and migrate towards the conductive band (CB) as displayed in Figure 6. This creates an electron-hole pair from the VB. On the CB, the electron interacts with the  $O_2$  and is reduced to form superoxide  $O_2^-$  since it is negatively charged. The electron-hole pairs from the VB undergo oxidation and interact with  $H_2O$  to form highly-oxidised hydroxyl ( $OH^-$ ) radicals. If the bandgap is broad, the electron hole-pairs start to recombine back to the VB. Therefore, radicals start attacking the pollutant and degrade the dye, remaining with environmentally friendly products which are  $H_2O$  and  $CO_2$  and less harmful minerals [93].

Various reports have shown that metal oxides such as ZnO and  $SnO_2$  have been used to degrade different organic dyes as semiconductors (Arakha et al., 2017); in Section 3.2, different metal oxides are discussed. Honardmand et al. [73] used jujube fruit for the synthesis of spherically shaped  $SnO_2$  NPs. From their study, a high degradation efficiency of 90 and 83% for MB and EBT was reported. Mahdhumita using *Abelmoschus esculentus musilage*-mediated ZnO NPs also reported the 100% degradation of Rhb dye in less than an hour using a Hg lamp. As stated, these materials do have great potential as photocatalysts; however, several limitations still need to be addressed.

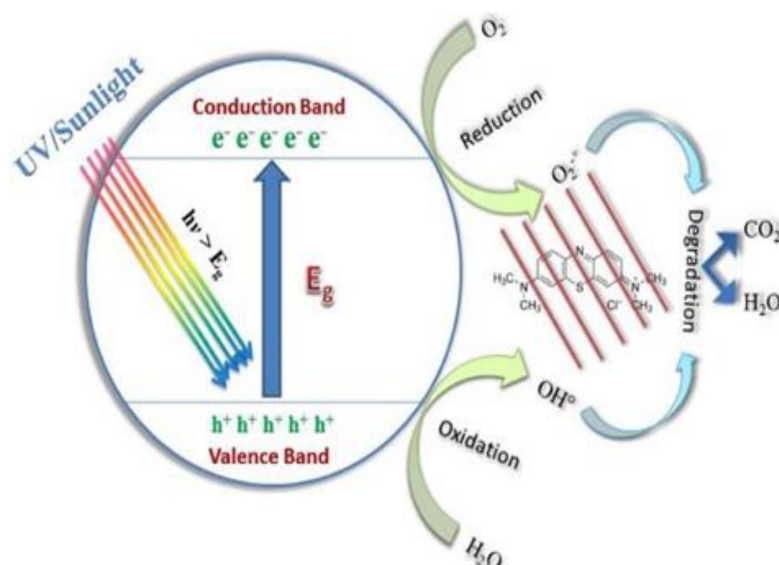


**Figure 6.** Mechanism of photocatalytic degradation [94].

### 3.2. Metal Oxides

Metal oxide nanoparticles such as ZnO, SnO<sub>2</sub> and TiO<sub>2</sub> are normally referred to as semiconductors due to their optical, chemical, physical and biomedical properties [95,96]. These materials have become prominent candidates due to the above-mentioned properties, hence they can be used for multifunctional applications such as drug delivery, photocatalysis and several other biological applications. They have been shown to have a higher adsorption capacity, thus assisting in cytotoxicity activities [97,98]. Furthermore, they have also been found to be competent in the removal of pathogens from wastewater because of their slow release of metal ions from the nanoparticles [99].

#### ZnO Nanoparticles

ZnO is an n-type semiconductor with a tetrahedral bonding configuration. It possesses a large bandgap as previously mentioned [100–102]. This means it is a high electro-optical device that can emit diodes, thus it can be used as a potential semiconductor material for the removal of various dyes. It also forms crystal structures in three different forms which are cubic rock salt, cubic zinc blend and hexagonal wurtzite structures as reported by Ong et al. [6] and which are represented as schematic structures in Figure 7a–c [103]. The rock salt structure forms at high pressure (Figure 7a), whereas cubic Zinc blende (Figure 7b) can be stabilized by growing ZnO on cubic substrates. Lastly, the ZnO hexagonal wurtzite (Figure 7c) crystal is the most prevalent form and the most thermodynamically stable at ambient conditions. Furthermore, the morphological cubic 3D structures have been reported by Yan et al. [104] and are presented in Figure 7d–e.

In addition to their photocatalytic ability, ZnO nanoparticles have also been reported to possess exceptional biological properties such as antibacterial, antifungal and antioxidant to mention a few [24]. The biomedical properties are due to the particle size, more especially, smaller particle sizes which have been shown to possess a higher surface area and better distribution of molecules [104]. The ZnO nanoparticles also possess photo-stability under ambient conditions, therefore, allowing for prolonged reaction time [105].

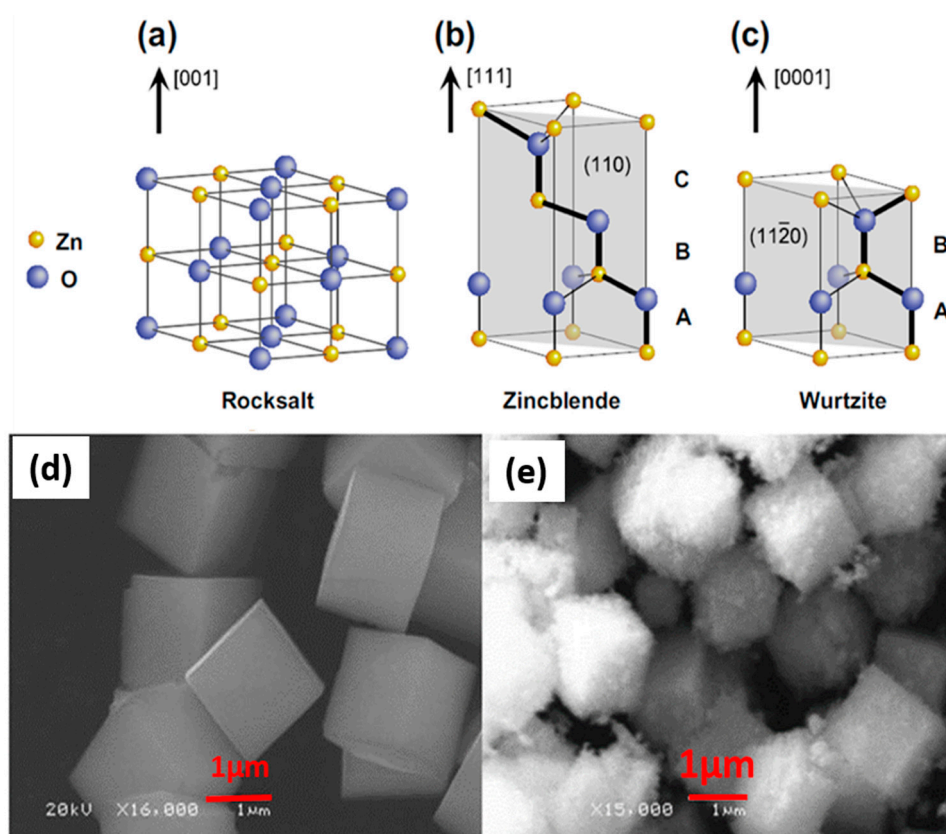


**Figure 7.** (a) Rock salt, (b) Zincblende, (c) Wurtzite crystal structure and (d,e) 3 D Cubic morphological structures of ZnO nanoparticles [6,104].

### 3.3. Green Chemistry

Green synthesis works similarly to chemical synthesis; however, the use of natural reductants is recommended. This synthesis method is based on the 12 green chemistry principles that were formulated to improve reaction efficiency, minimise the use of toxic solvents and processes and also ensure that minimal waste and hazardous materials are produced during synthesis. It provides controlled morphology, tunable particle size, well-dispersed particle sizes and the production of high-purity materials [93]. These green approaches involve the use of plant extracts (roots, leaves, stems, flowers and fruits), bio-waste materials (vegetables and fruit peel or skin), microbe-mediated (bacteria, fungi, yeast, algae) and enzymes synthetic methods (Figure 8) [106–108].

Amongst all these, plants have become the most desirable source of synthesizing ZnO NPs since they contribute to large-scale production as well as the production of stable, variable shape and size nanoparticles [109,110]. These plant extracts are also used as reducing, capping and stabilizing agents during the synthesis of nanoparticles [111]. Moreover, plant extracts are preferred over microbes since they are less toxic, inexpensive as compared to microorganisms' isolation, can be easily improved and lastly are easy to maintain and reduce the culture medium [112]. Fungus-based synthesis of nanoparticles has gained significant interest due to its widespread use in various disciplines [113,114]. As compared to bacteria, fungi can produce greater quantities of NPs since they can secrete larger amounts of proteins that directly result in the increased production of nanoparticles. Though fungi have some advantages, plants are still the preferred candidates, hence in the next section, we discuss the synthesis of green derived ZnO using plant extracts.

## Green synthesis

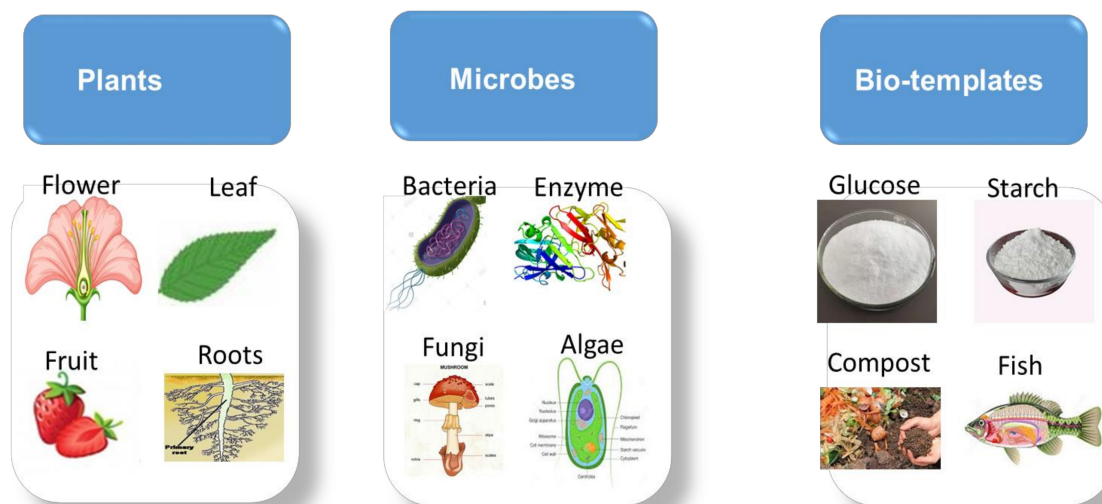


**Figure 8.** Various (plants, microbes and biotemplates) green synthesis sources.

### Green ZnO Using Plant Extracts

The use of plant extracts in the synthesis of ZnO nanoparticles is one of the most interesting methods since it is ecologically friendly, non-pathogenic, inexpensive and is not time-consuming, [115]. Special parts in plants such as the bark, root, stem, fruit, seed, peel, leaves and flower have been used for the synthesis of these ZnO NPs [116]. It has been stated that the key mechanism behind the use of plant extracts in the synthesis of ZnO NPs is a plant-assisted reduction in phytochemicals (Figure 9), which are chemicals produced by plants that can be used as capping and reducing agents. Primary phytochemicals which are considered during the synthesis of ZnO NPs include ketones, terpenoids, amides, flavones, carboxylic acids and aldehydes (Figure 9) [37,117,118]. To state how the formation of these particles takes place, it is not yet fully understood; however, the interaction between the metal ion and the phytochemicals does play a role.

Matinise et al., through the phytochemicals that were present in their *Moringa oleifera*, were able to explain the possible mechanism of formation for ZnO NPs [105]. Three possible compounds, phenolic acid, flavonoid and vitamin B, were used to demonstrate the three possible ways of solvating  $Zn^{2+}$  ions (Figure 10). Generally, the metal ions in the solution of the extract are altered by the oxidation of the present biological compounds via the free radicals. Thereafter, that action is followed by electrostatic attraction between free radicals and the metal precursor. One example includes L-ascorbic acid to dehydro L-ascorbic acid via free radical; then they interact with Zn ions from zinc acetate. In another study, Bopape et al., through the use of the *C. benghanlesis* plant extract which consisted of phytochemicals such as alkaloids, terpenoids, tannis etc., postulated that the mechanism begins with the addition of the precursor to the *C. benghnlesis* extract, which then results in the reduction in zinc ions ( $Zn^{2+}$ ) in addition to the nanoparticles' stabilisation.

Ashwini et al. [21], also through the use of their wild plant, *Acasia caesia*, which consisted of various phytochemicals such as fatty acids, alkaloids, tepernoids and phenols, were able to form ZnO nanoparticles with Zinc Nitrate as the precursor. In general, phenolics and flavonoids have shown their potential as capping and reducing agents. In the formation of ZnO NPs, in their study (Figure 11), they stated that phenolics have a high affinity to form complexes with other metals as they tend to act as good chelaters and in that process, the flavonoids are shown to be suitable capping agents of  $Zn^{2+}$  ions.

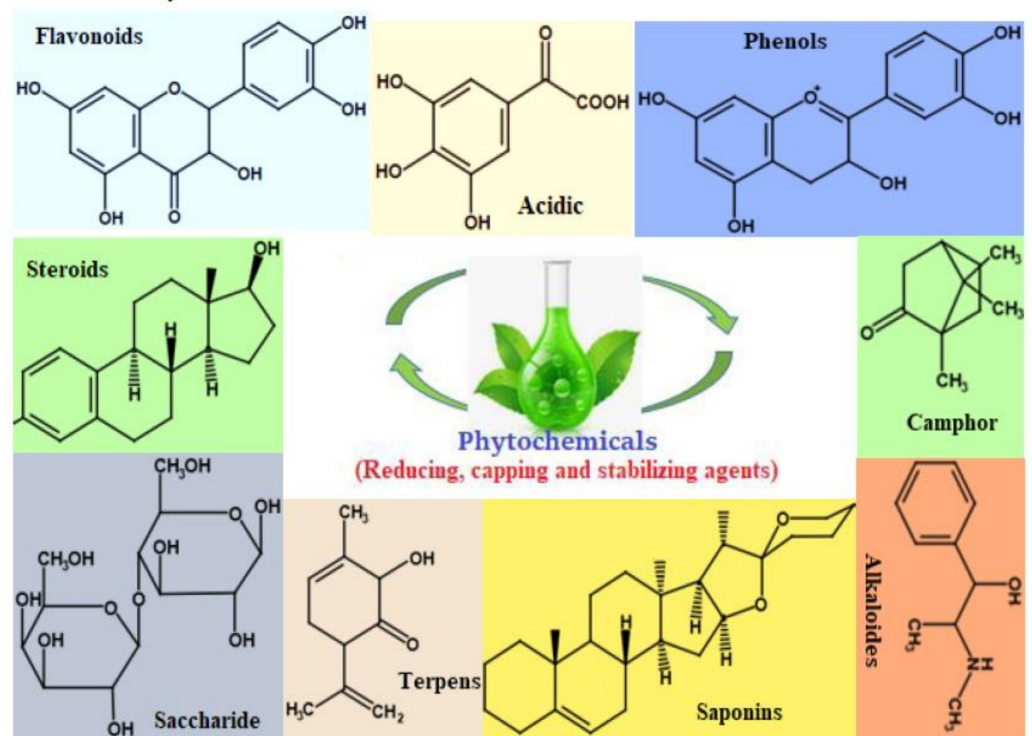


Figure 9. Some of the Phytochemicals present in different parts of plants [67].

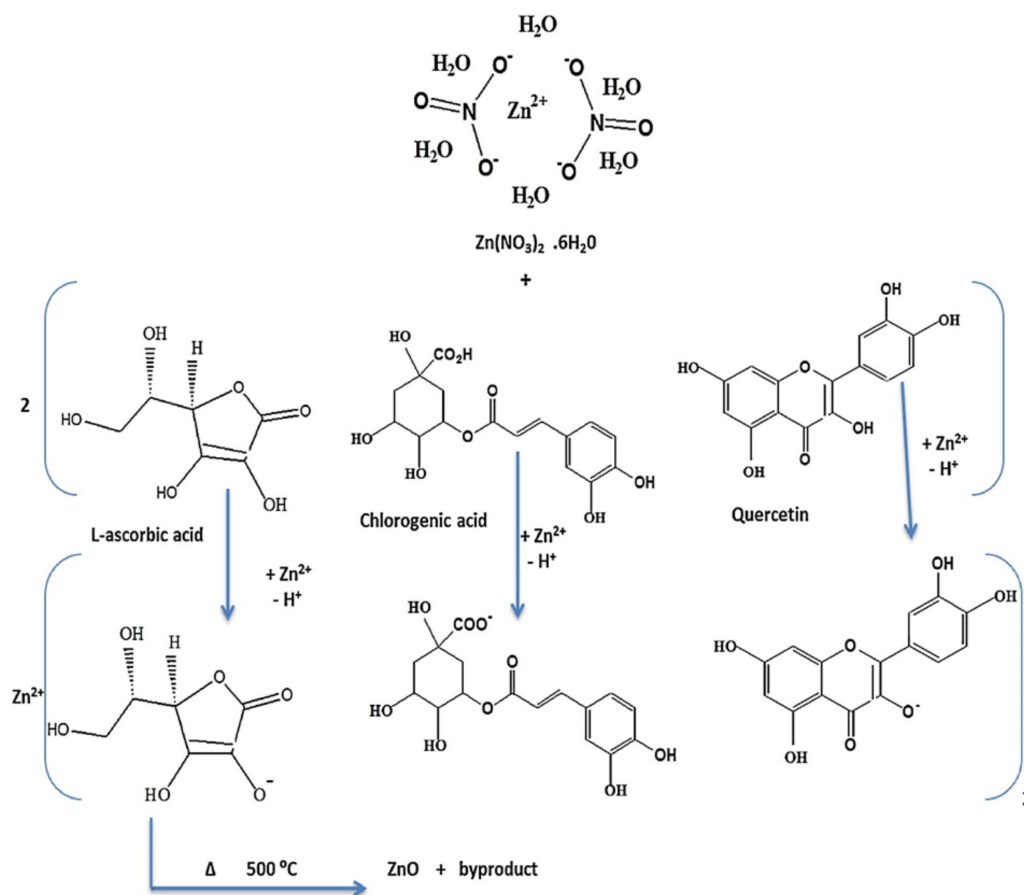
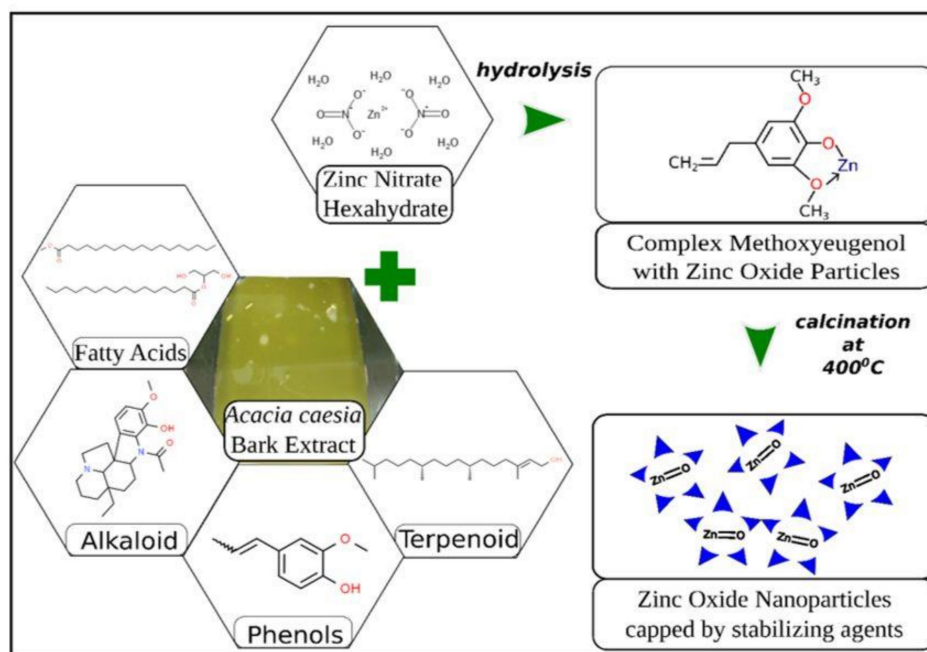


Figure 10. Mechanism of green synthesis of ZnO nanostructured material using plant [104].



**Figure 11.** The mechanism of formation of ZnO nanoparticles using *Acacia caesia* [21].

Saini et al. [26] synthesised ZnO NPs of blocks/bars of sizes of 40–120 nm using *Azadir indica* [26]. Umar et al. [119], using *Sapindus rarak* DC fruit extract, investigated the effect of pericap plant concentration and ammonia hydroxide on the morphology and size of the ZnO NPs. They found that polydispersed and irregularly shaped materials were formed, and furthermore, as the concentration increased, the particle sizes also became bigger as the average ranged from 50 to 95 nm. Bopape et al. [120] also investigated the effect of *Commelina benghlensis* plant concentration on the morphology and particle size of ZnO NPs. From their analysis, the morphology changed from flaky ZnO NPs at low concentrations with a broad size distribution of 20–140 nm to well-defined, spherically shaped, smaller (8–20 nm) particle sizes. Through the microwave-assisted synthesis, Raza et al. [40], using *Rumex dentatus* leaf extract, formed spherically shaped ZnO NPs with a particle size of 6.19 nm.

Different plant extracts were reported for the synthesis of ZnO nanoparticles, as exhibited in Table 3. From the table, it can be noted that a majority of the particles formed were of spherical morphological structures and a minority on the rods and hexagonal structures. This could have been due to the different salts used during the synthetic process. When the nitrate salt was used, mostly the spherical morphology was observed, as indicated in Table 3, whereas the rods and hexagonal structure were observed or rather reported when the chloride and the acetate salts were used. This could have been due to the interaction between the salt molecules and the phytochemicals. Having seen these factors contributing to their morphological structures, the authors are further reporting on the use of the ZnO as a photocatalyst for the degradation of dyes.

**Table 3.** Various plants used to synthesise ZnO nanoparticles.

Plant Source	Zinc Source	Shape	Size (nm)	Refs
<i>Azadir indica</i>	nitrate	Blocks/bars	40–100	[26]
<i>Rumex dentatus</i>	nitrate	spherical	6.19	[40]
<i>Moringa oleifera</i>	acetate	Spheres	40–45	[67]
<i>Commelina benghanlensis</i>	nitrate	Flakes/spheres	20–140	[120]
<i>Sapindus rarak</i> DC	nitrate	Polydispersed/irregular	50–95	[118]
<i>Pongamia pinnata</i>	nitrate	Spheres	26	[68]
<i>Aloe barbadensis</i>	nitrate	Spheres	25–40	[121]
<i>Prosopis forcta</i>	acetate	Spheres	20–25	[69]
<i>Camellia sinesis</i>	acetate	Rods	10–20	[121]
<i>Solanum nigrum</i>	nitrate	Quasi spherical	29–79	[72]
<i>Monsonia burkeana</i>	chloride	Hexagonal wurtzite	20	[100]
<i>Artocarpus heterophyllus</i>	chloride	Hexagonal	15–25	[73]
<i>Ceropegia candelabrum</i>	nitrate	-	12–35	[78]
<i>Ulva fasciata</i>	chloride	Rods	70	[79]
<i>Stevia</i>	acetate	Rectangular	10–90	[80]
<i>Bauhinia tomentosa</i>	sulfate		22–94	[81]
<i>Sutherlandia frutescens</i>	nitrate	Spherical	5–25	[25]

### 3.4. Green Derived ZnO as Photocatalyst for Dye Degradation

As previously mentioned, ZnO has been shown to be a good catalyst for the degradation of various pollutants [122–125]. In this section (Table 4) the ability of ZnO plant green derived materials is highlighted and its activity is observed. From the studies reported on, factors such as pH, light source, catalyst dosage, pollutant concentration and degradation time were noted [126,127]. In a study where green ZnO was formed from *Citrus maxima*, the effect of dosage (50–200 mg), concentration (5–20 ppm), pH (3–11) and the difference between sunlight and the UV light as a source was investigated. The study revealed that at the optimum conditions of 50 mg, 5 ppm, pH = 11 with the UV light, more than 90% of MB [94] was degraded. In a study by Ngoepe, whereby a similar amount of degradation time was provided (0.8 h) under the same UV light, but at a higher pollutant concentration (20 ppm) and a lower catalyst amount (20 mg), a big dip in the degradation of MB was noted, with only 48% of the dye degraded. This drastic change could have been due to the varying phytochemicals from the different plants, but more importantly, less than seven times the amount of catalyst was used at a much higher pollutant concentration. In that study, optimum conditions from the literature were used and that could have been the cause of the poor degradation efficiency. Moreover, the catalysts were not even reusable as the degradation effect was reduced with every cycle. Alshehri et al. [128] also had similar conditions to Ngoepe in terms of time, concentration and light source, however, they recorded a higher degradation efficiency against the RhB dye. Thus, it is always recommended that researchers always test various pollutants with their material to understand their multifunctional efficiency. For all the studies using Hg as a light source, a degradation efficiency of not less than 85% was noted irrespective of the time and pollutant used. Though they are efficient, they have been noted to be unsafe, hence the use of other light sources such as sunlight and UV-Vis light, which have been at the forefront. In a study by Bopape et al. [120], where various pollutants were tested and the effect of concentration was also investigated for the formation of their ZnO material, a maximum degradation of 83% at the highest concentration was noted, and this high efficiency was caused by the type of ZnO materials formed from morphology, and more importantly, the optical properties.

Through UV-vis, they were able to confirm the formation of their ZnO material. Because of the excitation mode of their surface plasmons, ZnO NPs give a characteristic absorbance band under the UV region, which is known to be dependent on the size of the nanoparticle. The Surface Plasmon Resonance (SPR) bands tend to undergo red shift or blue shift. In their study, a maximum absorption between 280 and 350 nm was noted, leading to a blue shift. From SPR, since the materials had foreign atoms in the lattice, the blue shift was caused by the existence of shallow levels within the band gap. They also noted that the OH radical species were mostly responsible for the degradation of their MB.

**Table 4.** Green synthesised metal oxides against different organic dyes.

Reductant	Organic Pollutant	Degradation Conditions	Efficiency (%)	Radiation Time (H)	Refs
<i>Citrus maxima</i> (Pomelo)	MB	5 ppm, 150 mg, pH = 11, UV light	Over 90	0.83	[94]
<i>Bacillus licheniformis</i>	MB	100 ppb, 0,25 g/L, Hg lamp,	85	1	[123]
<i>Vitis labuska</i>	MB	5 ppm, 100 mg, Hg Lamp, pH = 10	100	3	[97]
<i>Hagenia abyssinica</i>	MO	15 ppm, 40 mg, sunlight,	83	2	[124]
<i>Averrhoa carambola</i>	CR	100 ppm, 50 mg,	93	3	[125]
<i>Musa acuminata</i>	MB	$2 \times 10^{-5}$ M, 20 mg, UV light,	98	3	[126]
<i>Calliandra haematocephala</i>	MB	20 ppm, 50 mg, sunlight,	88	4.5	[127]
<i>Monsonia burkeana</i>	MB	20 ppm, 20 mg, UV light	48	0.8	[100]
<i>Trigonella foenum graecum</i>	MB	25 ppm, pH = 11, UV light	88	1.5	[128]
<i>Hippophae rhamnoides</i>	MG EY	10 ppm, 0.5 mg, UV linker	89 95	3	[129]
<i>Pithecellobium dulce</i>	MB	1 Mm, 15 mg, photoreactor	63	2	[130]
<i>Abelmoschus esculentus musilage</i>	Rhb	125 mg, Hg reactor	100	1	[131]
<i>Calotropis praera leaves</i>	MB	20 ppm, 1.5 g/L, UV light	81	1.4	[132]
<i>Eucalyptus globulus</i>	MB and MO	10 ppm, 30 mg, UV light	98.3	0.5	[133]
<i>Artocarpus gomezianus</i>	MB	5 ppm, 50 mg, sunlight & UV light, pH = 10	90	2	[134]
<i>Artocarpus heterophyllus</i>	CR	20 ppm, pH = 9	>90	1	[135]
<i>Plectranthus amboinicus</i>	MR	$1 \times 10^{-4}$ M, 20 mg, UV light	92	3	[136]
<i>Punica granatum</i>	R-250	5 ppm, 1 g/L,	93	3	[137]
<i>Terminalia chebula</i>		5 ppm, 1 g/L,		5	[138]
<i>Commelina benghanlensis</i>	MB	20 ppm, 30 mg, UV light, pH = 4	81	2	[139]
<i>Rueli tuberosa</i>	MB MG	10 ppm, 20 mg, UV light	94 92	2.5	[52]

MB = Methylene Blue; ECBT = Eriochrome Black; MR = Methylene Red; RhB = Rhodamine Blue; R-250 = Coomassie Brilliant Blue; Acid Yellow 23 = AY23; BB = Bismark Brown; MO = Methylene Orange; CR—Congo Red; AQ—Anthraquinone; AB = Acid Black; Phenol Red = Phenolsufonphathelin.

In summary, most of these results indicate that a higher degradation removal of dyes in longer irradiation times was achieved. Only a few studies displayed a higher degradation removal of dyes which were obtained in less than an hour. Above all, the presented reports confirm that ZnO is a good semiconductor, especially when used for the photocatalytic degradation process. In the next section, we will discuss its use as an antimicrobial agent.

### 3.5. Green Derived ZnO Antimicrobial Agent

Antibacterial activity is a process that monitors and controls bacterial growth by introducing antibacterial agents used to inhibit their growth [140]. ZnO is commonly used as an antibacterial agent, using methods such as plate count, disc diffusion and many others [11]. The mechanism of how metal oxides inhibit bacterial growth is exhibited in Figure 9.

The metal oxide as a treatment penetrates through the surface of the cell into the membrane. The dissolution of metal ions from the metal oxides starts to occur, and the metal cation is released. The released metal cation attacks the DNA and the enzymes within the cell. This leads to the structural distortion of the cell as indicated in Figure 12. This process does not permit cell growth and ultimately results in cell death [141]. In another study by Ashwini et al. [21], reactive oxygen species such as radical anions, hydroxyl radicals etc. were the main cause of the antibacterial activity as they were said to have interacted with the cells causing damage through oxidative stress. They also postulated that when the particles enter the cells via electrostatic forces and there is a loss of cell stability, cell death can also occur. Below we highlight a few studies showing the green derived antibacterial activity of these materials.

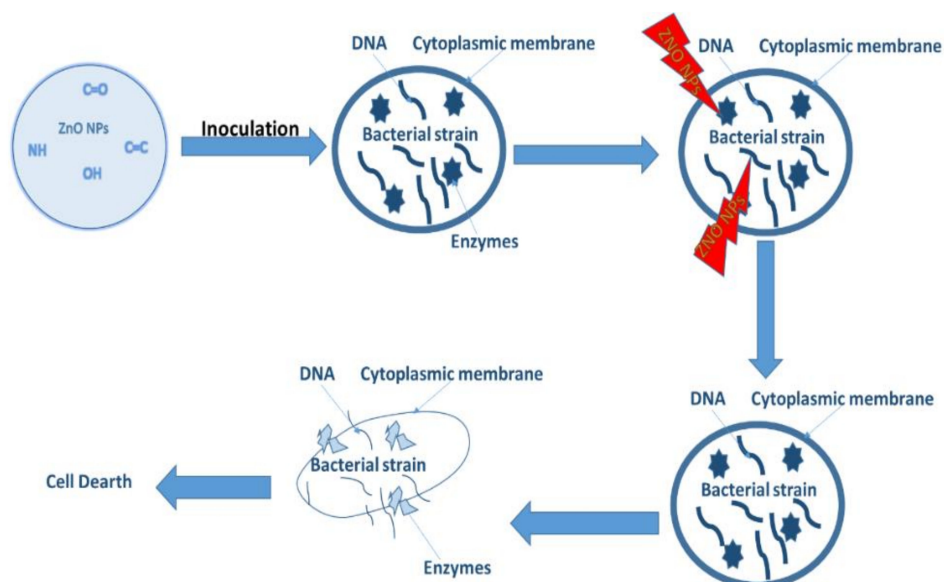


**Figure 12.** Schematic representation of the mechanism of action.

Chikkanna et al. [142] synthesised ZnO nanoparticles using goat and sheep faeces through dried faecal matter as natural reductants used to treat microbial strains. The materials using the disc diffusion method were potent against *Salmonella tryphimurium* (*S. typhi*) and *B. subtilis*, with a zone of inhibition of 1.16 nm and 1.08 nm. Sentikhumar and Thirumal [10], using ZnO-derived green tea *C. sinensis*, tested the antibacterial activity of various pollutants. From their analysis, they noted that gram-negative pollutants were more susceptible to the green materials and the gram-positive strains were somewhat resistant to the antibacterial efficiency. This could have been due to the phytochemicals found in the plant or the double layers the gram-positive strains consist of, thus making penetration harder. Another study was performed where *Aeromonas hydrophila* cells were used to synthesise ZnO nanoparticles for the antibacterial activity against *P. aeruginosa*. Using the well diffusion method, a maximum zone of inhibition of  $22 \pm 1.8$  mm was noted, thus indicating these materials were potent [143]. Mahlaule-Glory [11] tested the antibacterial efficiency of their material against both model and real water pollutants from various sources. Their material at concentrations of 0.01 mg/mL and above was able to damage more than 90% of the various strains. Additionally, they noted that when testing

against real water, depending on the source in some cases, the presence of the bacterial strains increased, leading to a conclusion that the phytochemicals in the plant extracts worked as feeders. In all the presented cases (Table 5), the preferred antibacterial method used was the disc diffusion method with *S. aureus* and *E. coli* as the pollutants of choice.

**Table 5.** Green ZnO NPs against natural pollutants.

Plant Extract	Shape	Size nm	Pollutants	Method	Inhibition	Refs
<i>Camellia Sinesis</i>	hexagonal	16	<i>K. pneumoniai</i> <i>E. coli</i> <i>P. aeruginosa</i> <i>S. aureus</i>	Agar-well diffusion	10.3 nm 3.3 nm 5.3 nm	[10]
<i>Rueli tuberosa</i>	Rod	40–50	<i>E. coli</i> , <i>S. aureus</i>	Agar-well diffusion	-	[52]
<i>Aspergillus niger</i>	Sphere	84–91	<i>E. coli</i> , <i>S. aureus</i>	Disc diffusion	12 nm 10 nm	[144]
<i>Citrus maxima</i>	Sphere	20	<i>E. coli</i> , <i>S. aureus</i> <i>K. aerogenes</i>	Disc diffusion	1.17 nm 3.53 nm 2.03 nm	[122]
<i>Dried faecal matter</i>	Oval	60–120	<i>S. typhimurium</i> <i>B. subtilis</i>	Disc diffusion	1.16 nm 1.08 nm	[142]
<i>Ceropegia candelabum</i>	Hexagonal	12–35	<i>E. coli</i> , <i>S. aureus</i> <i>B. sub</i>	Disc diffusion	0.00 mm 14.83 mm 10.66 mm	[145]
<i>Aloe vera</i>	Sphere	8–18	<i>E. coli</i> , <i>S. aureus</i> <i>P. aeruginosa</i>	Disc diffusion	22.1 mm 21.9 mm 18.8 mm	[146]
<i>Passiflora caerulea</i>	Hexagonal	16	<i>E. coli</i> , <i>S. aureus</i> <i>P. aeruginosa</i> <i>K. pneumonia</i>	Optical density measurement	8.33 mm 8.33 mm 7.33 mm 7.00 mm	[147]
<i>Aeronomas hydrophilia</i>	Oval and spherical	57	<i>A. flavus</i> <i>P. aeruginosa</i>	Disc diffusion	19 mm 22 mm	[143]
<i>Ailanthus altissima</i>	Sphere	5–18	<i>E. coli</i> , <i>S. aureus</i>	Disc diffusion	18 mm 20 mm	[148]
<i>Hageniaabyssinica</i>	Hexagonal	27	<i>E. coli</i> , <i>S. aureus</i> <i>S. epidermis</i> <i>K. pneumonia</i>	Disc diffusion	19 ± 1.0 19.33 ± 0.58 21 ± 1.0 18 ± 1.0	[124]
<i>Pithecellobium dulce</i>	Sphere	30	<i>A. flavus</i> <i>A. niger</i>	-	40% 43%	[130]
<i>Vitis labruska</i>	Hexagonal	20	<i>E. coli</i> , <i>S. aureus</i>	Disc diffusion	39.6 ± 0.28 30 ± 0.57	[97]

*E. coli* = *Escherichia Coli*; *S. aureus* = *Staphylococcus aureus*; *K. aerogenes* = *Klebsiella aerogenes*; *P. aeruginosa* = *Pseudomonas aeruginosa*; *S. try* = *Samonella tryphimurium*; *B. subtilis* = *Bacillus subtilis*; *K. pneumonia* = *Klesiella pneumonia*; *A. flavus* = *Asperigillus flavus*; *B. cereus* = *Bacillus cereus*; *S. epider* = *Staphylococcus epidermidts*; *A. niger* = *Aspergillus niger*; *C. abicans* = *Candida abicans*.

#### 4. Challenges of ZnO Material as Photocatalyst and Antimicrobial Agent

There are several challenges that are encountered by traditional semiconductors such as ZnO which are mostly due to the synthesis method or in their applications, especially in photocatalysis. As mentioned before, the use of toxic solvents has limited the use of these nanoparticles in several applications such as the biomedical field due to the toxicity of these materials. Moreover, the photocatalytic activity is influenced by the surface of the material, band gap and the photo-generation of the electron-holes of the nanostructures. Several parameters still need to be adhered to, to obtain suitable catalysts. Researchers have shown that coupling semiconductors with suitable electronic properties has been one of the methods used to improve the chemical properties of these semiconductors (Table 6). Increasing the charge separation of photogenerated electron-hole pairs generally increases

the photocatalytic efficiency. From the table indicated below, it is clear that there is a vast improvement in terms of degradation efficiency (more than 80%) when ZnO is coupled up with another metal. The bimetallic semiconductors even in other studies have shown properties such as optoelectronic and photocatalytic ability which can influence the separation and the recombination rate of the electron-hole pairs from the semiconductors. Depending on the valence and the conduction bands of the semiconductors, reducing the bandgap can extend the energy range of photoexcitation and thus give a better photodegradation of organic dyes. Moreover, other additional properties of coupling semiconductors include their low electrical resistance, faster charge transport, high electrical conductivity and higher recombination resistance.

**Table 6.** Green derived bimetallic NPs supporting ZnO for dye degradation.

Precursor	Plant	Shape	Size (nm)	Poll	Conc	% Removal	Time (min)	Refs
ZnO-CuO	<i>Calotropis gigantean</i>	Spheres	10–40	MB	5 ppm	98	105	[140]
Ag/ZnO	<i>Oak</i>	Sphere	19	BV3	100 $\mu$ M	94	120	[114]
Fe <sub>3</sub> O <sub>4</sub> /SiO <sub>2</sub> /ZnO	<i>Fructose</i>	Quazi sphere	38	CR	3 ppm	85	80	[44]
ZnO-SnO <sub>2</sub>	<i>Sutherlandia Frutescens</i>	Spheres	5–60	MB	20 ppm	88	120	[113]

## 5. Conclusions and Future Perspectives

This review has highlighted the different pollutants found in our water streams and their treatment strategies and limitations, photocatalysis as a treatment method of choice, the properties of ZnO nanoparticles and the use of these green derived materials as preferred catalysts for dye degradation and their effects as antibacterial agents. More needs to be done if these materials are to be synthesised at an industrial scale, such as controlling the extract amount and knowing the exact phytochemicals responsible for the synthesis. Importantly, factors such as doping with low bandgap metals, the formation of bimetallic nanocomposites and devising a means of increasing the surface area should not be ignored as these factors still need to be worked on even when using green derived nanoparticles. The biggest question we also need to ask ourselves as researchers is whether these green derived nanoparticles compete with conventionally synthesised materials in terms of activity, especially as photocatalysts.

**Author Contributions:** Conceptualization, N.C.H.-M. and L.M.M.-G.; formal analysis and investigation, N.C.H.-M. and L.M.M.-G. writing—original draft preparation, L.M.M.-G.; writing—review and editing L.M.M.-G. and N.C.H.-M.; supervision and funding acquisition, N.C.H.-M. All authors have read and agreed to the published version of the manuscript.

**Funding:** This research was funded by the National Research Foundation (Thuthuka) grant number TTK 117999.

**Data Availability Statement:** Not applicable.

**Acknowledgments:** The authors greatly acknowledge the contribution made by the DSI/NRF Centre of Excellence in Strong Materials. The NRF Thuthuka grant (UID: TTK-117999) is also acknowledged.

**Conflicts of Interest:** The authors declare no conflict of interest.

## References

- Meissner, R.; Steyn, M.; Moyo, E.; Shadung, J.; Masangane, W.; Nohayi, N.; Jacobs-Mata, I. South African local government perceptions of the state of water security. *Environ. Sci. Policy* **2018**, *87*, 112–127. [CrossRef]
- Reig, P.; Maddocks, A.; Gassert, F. *World's 36 Most Water-Stressed Countries*; World Resources Institute: Washington, DC, USA, 2013.
- Xiang, Y.; Wu, H.; Li, L.; Ren, M.; Qie, H.; Lin, A. A review of distribution and risk of pharmaceuticals and personal care products in the aquatic environment in China. *Ecotoxicol. Environ. Saf.* **2021**, *213*, 112044. [CrossRef] [PubMed]
- Cui, L.; Li, H.; Yang, K.; Zhu, L.; Xu, F.; Zhu, Y. Trends in Analytical Chemistry Raman biosensor and molecular tools for integrated monitoring of pathogens and antimicrobial resistance in wastewater. *Trends Anal. Chem.* **2021**, *143*, 116415. [CrossRef]

5. Lu, F.; Astruc, D. Nanomaterials for removal of toxic elements from water. *Coord. Chem. Rev.* **2018**, *356*, 147–164.
6. Ong, C.B.; Ng, L.Y.; Mohammad, A.W. A review of ZnO nanoparticles as solar photocatalysts: Synthesis, mechanisms and applications. *Renew. Sustain. Energy Rev.* **2018**, *81*, 536–551. [[CrossRef](#)]
7. Mohamed, A.A.; Abu-elghait, M.; Ahmed, N.E.; Salem, S.S. Eco-friendly Mycogenic Synthesis of ZnO and CuO Nanoparticles for In Vitro Antibacterial, Antibiofilm, and Antifungal Applications. *Biol. Trace Elem. Res.* **2021**, *199*, 2788–2799. [[CrossRef](#)] [[PubMed](#)]
8. Ayele, A.; Getachew, D.; Kamaraj, M.; Suresh, A. Phycoremediation of Synthetic Dyes: An Effective and Eco-Friendly Algal Technology for the Dye Abatement. *J. Chem.* **2021**, *2021*, 9923643. [[CrossRef](#)]
9. Bhuyan, B.; Paul, B.; Purkayastha, D.D.; Dhar, S.S.; Behera, S. Facile synthesis and characterization of zinc oxide nanoparticles and studies of their catalytic activity towards ultrasound-assisted degradation of metronidazole. *Mater. Lett.* **2016**, *168*, 158–162. [[CrossRef](#)]
10. Senthilkumar, S.R.; Sivakumar, T. Green tea (*Camellia sinensis*) mediated synthesis of zinc oxide (ZnO) nanoparticles and studies on their antimicrobial activities. *Int. J. Pharm. Pharm. Sci.* **2014**, *6*, 461–465.
11. Mahlaule-Glory, L.M.; Mbita, Z.; Ntsendwana, B.; Mathipa, M.M.; Mketi, N.; Hintsho-Mbita, N.C. ZnO nanoparticles via *Sutherlandia frutescens* plant extract: Physical and biological properties. *Mater. Res. Express* **2019**, *6*, 085006. [[CrossRef](#)]
12. Munyai, S.; Mahlaule-Glory, L.M.; Hintsho-Mbita, N.C. Green synthesis of Zinc sulphide (ZnS) nanostructures using *S. frutescens* plant extract for photocatalytic degradation of dyes and antibiotics. *Mater. Res. Express* **2022**, *9*, 015001. [[CrossRef](#)]
13. Selvaraj, V.; Karthika, T.S.; Mansiya, C.; Alagar, M. An over review on recently developed techniques, mechanisms and intermediate involved in the advanced azo dye degradation for industrial applications. *J. Mol. Struct.* **2021**, *1224*, 129195. [[CrossRef](#)]
14. Lee, K.M.; Lai, C.W.; Ngai, K.S.; Juan, J.C. Recent developments of zinc oxide based photocatalyst in water treatment technology: A review. *Water Res.* **2016**, *88*, 428–448. [[CrossRef](#)] [[PubMed](#)]
15. Zewde, D.; Geremew, B. Biosynthesis of ZnO nanoparticles using *Hagenia abyssinica* leaf extracts, their photocatalytic and antibacterials activities. *Environ. Pollut. Bioavailab.* **2022**, *34*, 224–235. [[CrossRef](#)]
16. Kulal, D.; Kodialbail, V.S. Visible light mediated photocatalytic dye degradation using Ag<sub>2</sub>O/AgO-TiO<sub>2</sub> nanocomposite synthesized by extracellular bacterial mediated synthesis—An eco-friendly approach for pollution abatement. *J. Environ. Chem. Eng.* **2021**, *9*, 105389. [[CrossRef](#)]
17. Roopan, S.M.; Elango, G.; Priya, D.D.; Asharani, I.V.; Kishore, B.; Vinayprabhakar, S.; Pragatheshwaran, N.; Mohanraj, K.; Harshpriya, R.; Shanavas, S.; et al. Sunlight mediated photocatalytic degradation of organic pollutants by statistical optimization of green synthesized NiO NPs as catalyst. *J. Mol. Liq.* **2019**, *293*, 111509. [[CrossRef](#)]
18. Pradinaud, C.; Northey, S.; Amor, B.; Bare, J.; Benini, L.; Berger, M.; Boulay, A.M.; Junqua, G.; Lathuillière, M.J.; Margni, M.; et al. Defining freshwater as a natural resource: A framework linking water use to the area of protection natural resources. *Int. J. Life Cycle Assess.* **2019**, *24*, 960–974. [[CrossRef](#)] [[PubMed](#)]
19. Wang, H.; Hecht, S.; Kline, D.; Leber, A.L. Staphylococcus aureus and methicillin resistance detection directly from pediatric samples using PCR assays with differential cycle threshold values for corroboration of methicillin resistance. *J. Microbiol. Methods* **2019**, *159*, 167–173. [[CrossRef](#)] [[PubMed](#)]
20. Stanley, H.O.; Ugboma, C.J.; Uzoaru, P.C. Investigations on Bacteriological Quality of Tap Water Sources within the University of Port Harcourt. *J. Adv. Microbiol.* **2019**, *16*, 1–5. [[CrossRef](#)]
21. Ashwini, J.; Aswathy, T.R.; Rahul, A.B.; Thara, G.M.; Nair, A.S. Synthesis and Characterization of Zinc Oxide Nanoparticles Using *Acacia caesia* Bark Extract and Its Photocatalytic and Antimicrobial Activities. *Catalysts* **2021**, *11*, 1507. [[CrossRef](#)]
22. Jeukens, J.; Freschi, L.; Kukavica-Ibrulj, I.; Emond-Rheault, J.G.; Allard, C.; Barbeau, J.; Cantin, A.; Charette, S.J.; Déziel, E.; Malouin, F.; et al. The *Pseudomonas aeruginosa* Population among Cystic Fibrosis Patients in Quebec, Canada: A disease hot spot without known epidemic isolates. *J. Clin. Microbiol.* **2019**, *57*, 1–3. [[CrossRef](#)] [[PubMed](#)]
23. Oves, M.; Aslam, M.; Rauf, M.A.; Qayyum, S.; Qari, H.A.; Khan, M.S.; Alam, M.Z.; Tabrez, S.; Pugazhendhi, A.; Ismail, I.M.I. Antimicrobial and anticancer activities of silver nanoparticles synthesized from the root hair extract of *Phoenix dactylifera*. *Mater. Sci. Eng. C* **2018**, *89*, 429–443. [[CrossRef](#)]
24. Vijayakumar, S.; Krishnakumar, C.; Arulmozhi, P.; Mahadevan, S.; Parameswari, N. Biosynthesis, characterization and antimicrobial activities of zinc oxide nanoparticles from leaf extract of *Glycosmis pentaphylla* (Retz.) DC. *Microb. Pathog.* **2018**, *116*, 44–48. [[CrossRef](#)]
25. Chai, Q.; Wu, Q.; Liu, T.; Tan, L.; Fu, C.; Ren, X.; Yang, Y.; Meng, X. Enhanced antibacterial activity of silica nanorattles with ZnO combination nanoparticles against methicillin-resistant *Staphylococcus aureus*. *Sci. Bull.* **2017**, *62*, 1207–1215. [[CrossRef](#)]
26. Saini, M.; Yadav, S.; Rani, N.; Mushtaq, A.; Rawat, S.; Sain, K.; Maity, D. Biosynthesized zinc oxide nanoparticles using seed and bark extract of *Azadirachta indica* for antibacterial, photocatalytic and supercapacitor applications. *Mater. Sci. Eng. B* **2022**, *282*, 115789. [[CrossRef](#)]
27. Sultana, S.; Mohammad, R.; Khan, Z.; Umar, K.; Ahmed, A.S.; Shahadat, M. SnO<sub>2</sub>-SrO based nanocomposites and their photocatalytic activity for the treatment of organic pollutants. *J. Mol. Struct.* **2015**, *1098*, 393–399. [[CrossRef](#)]
28. Bilińska, L.; Blus, K.; Gmurek, M.; Ledakowicz, S. Coupling of electrocoagulation and ozone treatment for textile wastewater reuse. *Chem. Eng. J.* **2019**, *358*, 992–1001. [[CrossRef](#)]
29. Sirelkhatim, A.; Mahmud, S.; Seeni, A.; Kaus, N.H.M.; Ann, L.C.; Bakhori, S.K.M.; Hasan, H.; Mohamad, D. Review on zinc oxide nanoparticles: Antibacterial activity and toxicity mechanism. *Nano-Micro Lett.* **2015**, *7*, 219–242. [[CrossRef](#)] [[PubMed](#)]

30. Agarwal, H.; Kumar, S.V.; Rajeshkumar, S. A review on green synthesis of zinc oxide nanoparticles—An eco-friendly approach. *Resour. Technol.* **2017**, *3*, 406–413. [[CrossRef](#)]
31. Rao, B.; Tang, R.-C. Green synthesis of silver nanoparticles with antibacterial activities using aqueous *Eriobotrya japonica* leaf extract. *Adv. Nat. Sci. Nanosci. Nanotechnol.* **2017**, *8*, 015014. [[CrossRef](#)]
32. Zhu, X.; Pathakoti, K.; Hwang, H.-M. Green synthesis of titanium dioxide and zinc oxide nanoparticles and their usage for antimicrobial applications and environmental remediation. In *Green Synthesis, Characterization and Applications of Nanoparticles*; Elsevier: Amsterdam, The Netherlands, 2019; pp. 223–263.
33. Umar, K.; Haque, M.M.; Mir, N.A.; Muneer, M.; Farooqi, I.H. Titanium Dioxide-mediated Photocatalysed Mineralization of Two Selected Organic Pollutants in Aqueous Suspensions. *J. Adv. Oxid. Technol.* **2016**, *16*, 252–260. [[CrossRef](#)]
34. Al-Asfar, A.; Zaheer, Z.; Aazam, E.S. Eco-friendly green synthesis of Ag@Fe bimetallic nanoparticles: Antioxidant, antimicrobial and photocatalytic degradation of bromothymol blue. *J. Photochem. Photobiol. B Biol.* **2018**, *185*, 143–152. [[CrossRef](#)] [[PubMed](#)]
35. Raja, S.; Ramesh, V.; Thivaharan, V. Green biosynthesis of silver nanoparticles using *Calliandra haematocephala* leaf extract, their antibacterial activity and hydrogen peroxide sensing capability. *Arab. J. Chem.* **2017**, *10*, 253–261. [[CrossRef](#)]
36. Ahmed, S.; Chaudhry, S.A.; Ikram, S. A review on biogenic synthesis of ZnO nanoparticles using plant extracts and microbes: A prospect towards green chemistry. *J. Photochem. Photobiol. B Biol.* **2017**, *166*, 272–284. [[CrossRef](#)]
37. Zaheer, Z. Biogenic synthesis, optical, catalytic, and in vitro antimicrobial potential of Ag-nanoparticles prepared using Palm date fruit extract. *J. Photochem. Photobiol. B Biol.* **2018**, *178*, 584–592. [[CrossRef](#)] [[PubMed](#)]
38. Mohanraj, R. Antimicrobial Activities of Metallic and Metal Oxide Nanoparticles From Plant Extracts. In *Antimicrobial Nanoarchitectonics*; Elsevier: Amsterdam, The Netherlands, 2017; pp. 83–100.
39. Hintsho, N.C.; Petrik, L.; Nechaev, A.; Titinchi, S.; Ndungu, P. Photo-catalytic activity of titanium dioxide carbon nanotube nano-composites modified with silver and palladium nanoparticles. *Appl. Catal. B Environ.* **2014**, *156*, 273.
40. Bar, H.; Bhui, D.K.; Sahoo, G.P.; Sarkar, P.; De, S.P.; Misra, A. Green synthesis of silver nanoparticles using latex of *Jatropha curcas*. *Colloids Surf. A Physicochem. Eng. Asp.* **2009**, *339*, 134–139. [[CrossRef](#)]
41. Nazir, A.; Raza, M.; Abbas, M.; Abbas, S.; Ali, A.; Ali, Z.; Younas, U.; Al-Mijalli, S.H.; Iqbal, M. Microwave assisted green synthesis of ZnO nanoparticles using *Rumex dentatus* leaf extract: Photocatalytic and antibacterial potential evaluation. *Z. Phys. Chem.* **2022**. [[CrossRef](#)]
42. Vijayakumar, S.; Vinoj, G.; Malaikozhundan, B.; Shanthi, S.; Vaseeharan, B. Plectranthus amboinicus leaf extract mediated synthesis of zinc oxide nanoparticles and its control of methicillin resistant *Staphylococcus aureus* biofilm and blood sucking mosquito larvae. *Spectrochim. Acta Part A Mol. Biomol. Spectrosc.* **2015**, *137*, 886–891. [[CrossRef](#)]
43. Barbosa, M.O.; Moreira, N.F.F.; Ribeiro, A.R.; Pereira, M.F.R.; Silva, A.M.T. Occurrence and removal of organic micropollutants: An overview of the watch list of EU Decision 2015/495. *Water Res.* **2016**, *94*, 257–279. [[CrossRef](#)] [[PubMed](#)]
44. Ali, H.R.; Hassaan, M.A. Applications of Bio-waste Materials as Green Synthesis of Nanoparticles and Water Purification. *Adv. Mater.* **2017**, *6*, 85.
45. Sewu, D.D.; Lee, D.S.; Woo, S.H.; Kalderis, D. Decolorization of triarylmethane dyes, malachite green, and crystal violet, by sewage sludge biochar: Isotherm, kinetics, and adsorption mechanism comparison. *Korean J. Chem. Eng.* **2021**, *38*, 531–539. [[CrossRef](#)]
46. İlkez, B.A.; Beceren, Y.İ.; Candan, C. An Approach to Estimate Dye Concentration of Domestic Washing Machine Wastewater. *Autex Res. J.* **2021**, *21*, 172–181.
47. Akbari, A.; Sabouri, Z.; Hosseini, H.A.; Hashemzadeh, A.; Khatami, M.; Darroudi, M. Effect of nickel oxide nanoparticles as a photocatalyst in dyes degradation and evaluation of effective parameters in their removal from aqueous environments. *Inorg. Chem. Commun.* **2020**, *115*, 107867. [[CrossRef](#)]
48. Munyai, S.; Hintsho-Mbita, N.C. Green derived metal sulphides as photocatalysts for waste water treatment. A review. *Curr. Res. Green Sustain. Chem.* **2021**, *4*, 100163. [[CrossRef](#)]
49. Shahnaz, T.; Bedadeep, D.; Narayanasamy, S. Investigation of the adsorptive removal of methylene blue using modified nanocellulose. *Int. J. Biol. Macromol.* **2022**, *200*, 162–171. [[CrossRef](#)]
50. Noman, M.; Shahid, M.; Ahmed, T.; Niazi, M.B.K.; Hussain, S.; Song, F.; Manzoor, I. Use of biogenic copper nanoparticles synthesized from a native *Escherichia sp.* as photocatalysts for azo dye degradation and treatment of textile effluents. *Environ. Pollut.* **2020**, *257*, 113514. [[CrossRef](#)] [[PubMed](#)]
51. Kumaravelan, S.; Seshadri, S.; Suresh, R.; Ravichandran, K.; Sathishkumar, P.; Shanthaseelan, K.; Suganthi, N. Effect of Zn dopant on SnO<sub>2</sub> nano-pyramids for photocatalytic degradation. *Chem. Phys. Lett.* **2021**, *769*, 138352. [[CrossRef](#)]
52. Mahdavi, K.; Zinatloo-Ajabshir, S.; Yousif, Q.A.; Salavati-Niasari, M. Enhanced photocatalytic degradation of toxic contaminants using Dy<sub>2</sub>O<sub>3</sub>-SiO<sub>2</sub> ceramic nanostructured materials fabricated by a new, simple and rapid sonochemical approach. *Ultrason. Sonochem.* **2022**, *82*, 105892. [[CrossRef](#)] [[PubMed](#)]
53. Vasantharaj, S.; Sathiyavimal, S.; Senthilkumar, P.; Kalpana, V.N.; Rajalakshmi, G.; Alsehli, M.; Elfasakhany, A.; Pugazhendhi, A. Enhanced photocatalytic degradation of water pollutants using bio-green synthesis of zinc oxide nanoparticles (ZnO NPs). *J. Environ. Chem. Eng.* **2021**, *9*, 105772. [[CrossRef](#)]
54. Haque, A.; Bin Islam, K.; Mahbub, S.; Khan, J.M.; Hossian, J.; Hoque, A.; Halim, M.A.; Rahman, M.M.; Ahmad, A.; Ahmed, M.Z. Impact of ethanol and NaCl on the acid yellow dye mediated self-aggregation of sodium dodecyl sulfate: A combined investigation by conductivity and molecular dynamics simulation. *J. Mol. Liq.* **2022**, *345*, 117819.

55. Raja, A.; Ashokkumar, S.; Marthandam, R.P.; Jayachandiran, J.; Khatiwada, C.P.; Kaviyarasu, K.; Raman, R.G.; Swaminathan, M. Eco-friendly preparation of zinc oxide nanoparticles using *Tabernaemontana divaricata* and its photocatalytic and antimicrobial activity. *J. Photochem. Photobiol. B Biol.* **2018**, *181*, 53–58. [[CrossRef](#)] [[PubMed](#)]
56. Aarathi, T.; Madras, G. Photocatalytic degradation of rhodamine dyes with nano-TiO<sub>2</sub>. *Ind. Eng. Chem. Res.* **2007**, *46*, 7–14. [[CrossRef](#)]
57. Jaitpal, S.; Naik, P.; Chakraborty, S.; Banerjee, S.; Paul, D. Exploring the concentration-dependent transport and the loss of rhodamine B, tartrazine, methylene blue, and amaranth dyes in common paperfluidic substrates. *Results Surf. Interfaces* **2022**, *6*, 100034. [[CrossRef](#)]
58. Priyanka, U.; Lens, P.N.L. Light driven *Aspergillus niger*-ZnS nanobiohybrids for degradation of methyl orange. *Chemosphere* **2022**, *298*, 134162. [[CrossRef](#)]
59. Cui, M.; Xie, Z.; Wang, M.; Zhang, X. Methyl orange-crosslinked polypyrrole hydrogel enabled N, O, S co-doped porous carbon for highly sensitive determination of three redox-active biomolecules. *J. Electroanal. Chem.* **2022**, *913*, 116282. [[CrossRef](#)]
60. Yadav, A.; Dindorkar, S.S. Adsorption behaviour of hexagonal boron nitride nanosheets towards cationic, anionic and neutral dyes: Insights from first principle studies. *Colloids Surfaces A Physicochem. Eng. Asp.* **2022**, *640*, 128509. [[CrossRef](#)]
61. Vela-Carrillo, A.Z.; Martínez, R.J.; Godínez, L.A.; Pérez-Bueno, J.D.J.; Espejel-Ayala, F.; Robles, I. Study of chemical, kinetic, and theoretical sorption properties of activated carbons obtained from agroindustrial origin: Comparison of anionic and cationic model molecules. *Biomass Convers. Biorefin.* **2022**, *12*, 1–18. [[CrossRef](#)]
62. Attallah, O.A.; Al-Ghobashy, M.A.; Nebsen, M.; Salem, M.Y. Removal of cationic and anionic dyes from aqueous solution with magnetite/pectin and magnetite/silica/pectin hybrid nanocomposites: Kinetic, isotherm and mechanism analysis. *RSC Adv.* **2016**, *6*, 11461–11480. [[CrossRef](#)]
63. Karaman, C.; Karaman, O.; Show, P.L.; Karimi-Maleh, H.; Zare, N. Congo red dye removal from aqueous environment by cationic surfactant modified-biomass derived carbon: Equilibrium, kinetic, and thermodynamic modeling, and forecasting via artificial neural network approach. *Chemosphere* **2022**, *290*, 133346. [[CrossRef](#)]
64. Jiménez-Mancilla, N.P.; Aranda-Lara, L.; Morales-Ávila, E.; Camacho-López, M.A.; Ocampo-García, B.E.; Torres-García, E.; Estrada-Guadarrama, J.A.; Santos-Cuevas, C.L.; Isaac-Olivé, K. Electron transfer reactions in rhodamine: Potential use in photodynamic therapy. *J. Photochem. Photobiol. A Chem.* **2021**, *409*, 113131. [[CrossRef](#)]
65. Rout, L.; Kumar, A.; Satish, K.; Achary, L.; Barik, B.; Dash, P. Ionic liquid assisted combustion synthesis of ZnO and its modification by Au–Sn bimetallic nanoparticles: An efficient photocatalyst for degradation of organic contaminants. *Mater. Chem. Phys.* **2019**, *232*, 339–353. [[CrossRef](#)]
66. Brezová, V.; Čeppan, M.; Veselý, M.; Lapčík, L. Photocatalytic oxidation of 2,6-dichloroindophenol in the titanium dioxide aqueous suspension. *Chem. Papers* **1991**, *45*, 233–246.
67. Rajan, P.I.; Vijaya, J.J.; Jesudoss, S.K.; Kaviyarasu, K.; Kennedy, L.J.; Jothiramalingam, R.; Al-Lohedan, H.A.; Vaali-Mohammed, M.A. Green-fuel-mediated synthesis of self-assembled NiO nano-sticks for dual applications-photocatalytic activity on Rose Bengal dye and antimicrobial action on bacterial strains. *Mater. Res. Express* **2017**, *4*, 100375. [[CrossRef](#)]
68. Zeebaree, A.Y.S.; Rashid, R.F.; Zebari, O.I.H.; Albarwry, A.J.S.; Ali, A.F.; Zebari, A.Y.S. Sustainable engineering of plant-synthesized TiO<sub>2</sub> nanocatalysts: Diagnosis, properties and their photocatalytic performance in removing of Methylene Blue dye from effluent. A review. *Curr. Res. Green Sustain. Chem.* **2022**, *5*, 100312.
69. Liu, X.-B.; Lu, H.-Y.; Huang, W.-M.; Kong, H.-S.; Ren, X.-B.; Lin, H.-B. Electrochemical Degradation of Nitrobenzene. *Curr. Org. Chem.* **2012**, *16*, 1967–1971. [[CrossRef](#)]
70. Mohanty, S.S.; Kumar, A. Enhanced degradation of anthraquinone dyes by microbial monoculture and developed consortium through the production of specific enzymes. *Sci. Rep.* **2021**, *11*, 7678.
71. Yang, W.; Li, Q.; Guo, S.; Sun, S.; Tang, A.; Liu, H.; Liu, Y. Rational design of *Aspergillus flavus* A5p1-immobilized cell system to enhance the decolorization of reactive blue 4 (RB4). *Chin. J. Chem. Eng.* **2022**. [[CrossRef](#)]
72. Orooji, Y.; Mohassel, R.; Amiri, O.; Sobhani, A.; Salavati-Niasari, M. Gd<sub>2</sub>ZnMnO<sub>6</sub>/ZnO nanocomposites: Green sol-gel auto-combustion synthesis, characterization and photocatalytic degradation of different dye pollutants in water. *J. Alloys Compd.* **2020**, *835*, 155240. [[CrossRef](#)]
73. Honarmand, M.; Golmohammadi, M.; Naeimi, A. Biosynthesis of tin oxide (SnO<sub>2</sub>) nanoparticles using jujube fruit for photocatalytic degradation of organic dyes. *Adv. Powder Technol.* **2019**, *30*, 1551–1557. [[CrossRef](#)]
74. Khani, R.; Roostaei, B.; Bagherzade, G.; Moudi, M. Green synthesis of copper nanoparticles by fruit extract of *Ziziphus spinachristi* (L.) Willd.: Application for adsorption of triphenylmethane dye and antibacterial assay. *J. Mol. Liq.* **2018**, *255*, 541–549. [[CrossRef](#)]
75. Kanagamani, K.; Muthukrishnan, P.; Saravanakumar, K.; Shankar, K.; Kathiresan, A. Photocatalytic degradation of environmental perilous gentian violet dye using leucaena-mediated zinc oxide nanoparticle and its anticancer activity. *Rare Met.* **2019**, *38*, 277–286. [[CrossRef](#)]
76. He, Y.; Li, X.; Wang, J.; Yang, Q.; Yao, B.; Zhao, Y.; Zhao, A.; Sun, W.; Zhang, Q. Synthesis, characterization and evaluation cytotoxic activity of silver nanoparticles synthesized by Chinese herbal *Cornus officinalis* via environment friendly approach. *Environ. Toxicol. Pharmacol.* **2017**, *56*, 56–60. [[CrossRef](#)] [[PubMed](#)]

77. Cai, D.; Li, X.; Chen, J.; Jiang, X.; Ma, X.; Sun, J.; Tian, L.; Vidyarthi, S.K.; Xu, J.; Pan, Z.; et al. A comprehensive review on innovative and advanced stabilization approaches of anthocyanin by modifying structure and controlling environmental factors. *Food Chem.* **2022**, *366*, 130611. [[CrossRef](#)] [[PubMed](#)]
78. De León-Condés, C.A.; Roa-Morales, G.; Martínez-Barrera, G.; Menchaca-Campos, C.; Bilyeu, B.; Balderas-Hernández, P.; Ureña-Núñez, F.; Toledo-Jaldin, H.P. Sulfonated and gamma-irradiated waste expanded polystyrene with iron oxide nanoparticles, for removal of indigo carmine dye in textile wastewater. *Heliyon* **2019**, *5*, e02071. [[CrossRef](#)]
79. Slavin, Y.N.; Asnis, J.; Häfeli, U.O.; Bach, H. Metal nanoparticles: Understanding the mechanisms behind antibacterial activity. *J. Nanobiotechnol.* **2017**, *15*, 1–20. [[CrossRef](#)]
80. Aisida, S.O.; Ugwoke, E.; Uwais, A.; Iroegbu, C.; Botha, S.; Ahmad, I.; Maaza, M.; Ezema, F.I. Incubation period induced biogenic synthesis of PEG enhanced Moringa oleifera silver nanocapsules and its antibacterial activity. *J. Polym. Res.* **2019**, *26*, 1–11. [[CrossRef](#)]
81. Ishwarya, R.; Vaseeharan, B.; Kalyani, S.; Banumathi, B.; Govindarajan, M.; Alharbi, N.S.; Kadaikunnan, S.; Al-anbr, M.N.; Khaled, J.M.; Benelli, G. Facile green synthesis of zinc oxide nanoparticles using *Ulva lactuca* seaweed extract and evaluation of their photocatalytic, antibiofilm and insecticidal activity. *J. Photochem. Photobiol. B Biol.* **2018**, *178*, 249–258. [[CrossRef](#)] [[PubMed](#)]
82. Padalia, H.; Moteriya, P.; Chanda, S. Green synthesis of silver nanoparticles from marigold flower and its synergistic antimicrobial potential. *Arab. J. Chem.* **2015**, *8*, 732–741. [[CrossRef](#)]
83. Elhadi, D.; Lv, L.; Jiang, X.R.; Wu, H.; Chen, G.Q. CRISPRi engineering *E. coli* for morphology diversification. *Metab. Eng.* **2016**, *38*, 358–369. [[CrossRef](#)]
84. Babu, B.; Cho, M.; Byon, C.; Shim, J. One pot synthesis of Ag-SnO<sub>2</sub> quantum dots for highly enhanced sunlight-driven photocatalytic activity. *J. Alloys Compd.* **2018**, *731*, 162–171. [[CrossRef](#)]
85. Ligaray, M.; Kim, N.H.; Park, S.; Park, J.S.; Park, J.; Kim, Y.; Cho, K.H. Energy projection of the seawater battery desalination system using the reverse osmosis system analysis model. *Chem. Eng. J.* **2020**, *395*, 125082. [[CrossRef](#)]
86. Haq, S.; Rehman, W.; Waseem, M.; Shah, A.; Khan, A.R.; Rehman, M.U.; Ahmad, P.; Khan, B.; Ali, G. Green synthesis and characterization of tin dioxide nanoparticles for photocatalytic and antimicrobial studies. *Mater. Res. Express* **2020**, *7*, 025012. [[CrossRef](#)]
87. Moreira, V.R.; Lebron, Y.A.R.; da Silva, M.M.; de Souza Santos, L.V.; Jacob, R.S.; de Vasconcelos, C.K.B.; Viana, M.M. Graphene oxide in the remediation of norfloxacin from aqueous matrix: Simultaneous adsorption and degradation process. *Environ. Sci. Pollut. Res.* **2020**, *27*, 34513–34528. [[CrossRef](#)] [[PubMed](#)]
88. Shabani, M.; Younesi, H.; Pontié, M.; Rahimpour, A.; Rahimnejad, M.; Zinatizadeh, A.A. A critical review on recent proton exchange membranes applied in microbial fuel cells for renewable energy recovery. *J. Clean. Prod.* **2020**, *264*, 121446. [[CrossRef](#)]
89. Saravanan, A.; Senthil Kumar, P.; Jeevanantham, S.; Karishma, S.; Tajsabreen, B.; Yaashikaa, P.R.; Reshma, B. Effective water/wastewater treatment methodologies for toxic pollutants removal: Processes and applications towards sustainable development. *Chemosphere* **2021**, *280*, 130595. [[CrossRef](#)]
90. Mohamed Noor, M.H.; Ngadi, N.; Mohammed Inuwa, I.; Opotu, L.A.; Mohd Nawawi, M.G. Synthesis and application of polyacrylamide grafted magnetic cellulose flocculant for palm oil wastewater treatment. *J. Environ. Chem. Eng.* **2020**, *8*, 104014. [[CrossRef](#)]
91. Saravanan, M.; Gopinath, V.; Chaurasia, M.K.; Syed, A.; Ameen, F.; Purushothaman, N. Green synthesis of anisotropic zinc oxide nanoparticles with antibacterial and cytofriendly properties. *Microb. Pathog.* **2018**, *115*, 57–63. [[CrossRef](#)] [[PubMed](#)]
92. Paździor, K.; Wrębiak, J.; Klepacz-Smółka, A.; Gmurek, M.; Bilińska, L.; Kos, L.; Sójka-Ledakowicz, J.; Ledakowicz, S. Influence of ozonation and biodegradation on toxicity of industrial textile wastewater. *J. Environ. Manage.* **2017**, *195*, 166–173. [[CrossRef](#)] [[PubMed](#)]
93. Paździor, K.; Klepacz-Smółka, A.; Ledakowicz, S.; Sójka-Ledakowicz, J.; Mrozińska, Z.; Żyła, R. Integration of nanofiltration and biological degradation of textile wastewater containing azo dye. *Chemosphere* **2009**, *75*, 250–255. [[CrossRef](#)] [[PubMed](#)]
94. Begum, S.; Devi, T.B.; Ahmaruzzaman, M. L-lysine monohydrate mediated facile and environment friendly synthesis of SnO<sub>2</sub> nanoparticles and their prospective applications as a catalyst for the reduction and photodegradation of aromatic compounds. *J. Environ. Chem. Eng.* **2016**, *4*, 2976–2989. [[CrossRef](#)]
95. Pavithra, N.S.; Lingaraju, K.; Raghu, G.K.; Nagaraju, G. Citrus maxima (Pomelo) juice mediated eco-friendly synthesis of ZnO nanoparticles: Applications to photocatalytic, electrochemical sensor and antibacterial activities. *Spectrochim. Acta Part A Mol. Biomol. Spectrosc.* **2017**, *185*, 11–19. [[CrossRef](#)] [[PubMed](#)]
96. Al-Hamdi, A.M.; Rinner, U.; Sillanpää, M. Tin dioxide as a photocatalyst for water treatment: A review. *Process. Saf. Environ. Prot.* **2017**, *107*, 190–205. [[CrossRef](#)]
97. Varghese, E.; George, M. Green Synthesis of Zinc Oxide Nanoparticles. *Int. J. Adv. Res. Sci. Eng.* **2015**, *4*, 307–314.
98. Mostoni, S.; Pifferi, V.; Falciola, L.; Meroni, D.; Pargoletti, E.; Davoli, E.; Cappelletti, G. Tailored routes for home-made Bi-doped ZnO nanoparticles. Photocatalytic performances towards o-toluidine, a toxic water pollutant. *J. Photochem. Photobiol. A Chem.* **2017**, *332*, 534–545. [[CrossRef](#)]
99. Arakha, M.; Roy, J.; Nayak, P.S.; Mallick, B.; Jha, S. Zinc oxide nanoparticle energy band gap reduction triggers the oxidative stress resulting into autophagy-mediated apoptotic cell death. *Free Radic. Biol. Med.* **2017**, *110*, 42–53. [[CrossRef](#)] [[PubMed](#)]
100. Davar, F.; Majedi, A.; Mirzaei, A. Green synthesis of ZnO nanoparticles and its application in the degradation of some dyes. *J. Am. Ceram. Soc.* **2015**, *98*, 1739–1746. [[CrossRef](#)]

101. Ngoepe, N.M.; Mbita, Z.; Mathipa, M.; Mketi, N.; Ntsendwana, B.; Hintsho-Mbita, N.C. Biogenic synthesis of ZnO nanoparticles using *Monsonia burkeana* for use in photocatalytic, antibacterial and anticancer applications. *Ceram. Int.* **2018**, *44*, 16999–17006. [[CrossRef](#)]
102. Shenoy, S.; Tarafder, K.; Sridharan, K. Bimetallic nanoparticles grafted ZnO hierarchical structures as efficient visible light driven photocatalyst: An experimental and theoretical study. *J. Mol. Struct.* **2021**, *1236*, 130355. [[CrossRef](#)]
103. Abbas, A.M.; Abid, M.A.; Abbas, K.N.; Aziz, W.J.; Salim, A.A. Photocatalytic Activity of Ag-ZnO Nanocomposites Integrated Essential Ginger Oil Fabricated by Green Synthesis Method. *J. Phys. Conf. Ser.* **2021**, *1892*, 012005. [[CrossRef](#)]
104. Yan, Y.; Liu, J.; Zhang, H.; Song, D.; Li, J.; Yang, P.; Zhang, M.; Wang, J. One-pot synthesis of cubic ZnSnO<sub>3</sub>/ZnO heterostructure composite and enhanced gas-sensing performance. *J. Alloys Compd.* **2019**, *780*, 193–201. [[CrossRef](#)]
105. Matinise, N.; Fuku, X.G.; Kaviyarasu, K.; Mayedwa, N.; Maaza, M. Applied Surface Science ZnO nanoparticles via *Moringa oleifera* green synthesis: Physical properties & mechanism of formation. *Appl. Surf. Sci.* **2017**, *406*, 339–347.
106. Ahmed, T.; Wu, Z.; Jiang, H.; Luo, J.; Noman, M.; Shahid, M.; Manzoor, I.; Allemailem, K.S.; Alrumaihi, F.; Li, B. Bioinspired Green Synthesis of Zinc Oxide Nanoparticles from a Native *Bacillus cereus* Strain RNT6: Characterization and Antibacterial Activity against Rice Panicle Blight Pathogens *Burkholderia glumae* and *B. gladioli*. *Nanomaterials* **2021**, *11*, 884. [[CrossRef](#)] [[PubMed](#)]
107. Dhanemozhi, A.C.; Rajeswari, V.; Sathyajothi, S. Green Synthesis of Zinc Oxide Nanoparticle Using Green Tea Leaf Extract for Supercapacitor Application. *Mater. Today Proc.* **2017**, *4*, 660–667. [[CrossRef](#)]
108. Jiménez-Rosado, M.; Gomez-Zavaglia, A.; Guerrero, A.; Romero, A. Green synthesis of ZnO nanoparticles using polyphenol extracts from pepper waste (*Capiscum annuum*). *J. Clean. Prod.* **2022**, *350*, 131541. [[CrossRef](#)]
109. Mercedes, R. The Health Benefits of Fruits and Vegetables. *Foods* **2020**, *9*, 1–4.
110. Kumar, I.; Mondal, M.; Sakthivel, N. Green synthesis of phytogenic nanoparticles. *Green Synth. Charact. Appl. Nanopart.* **2019**, *37–73*.
111. Hussain, I.; Singh, N.B.; Singh, A.; Singh, H.; Singh, S.C. Green synthesis of nanoparticles and its potential application. *Biotechnol. Lett.* **2016**, *38*, 545–560. [[CrossRef](#)]
112. Kharissova, O.V.; Dias, H.V.R.; Kharisov, B.I.; Pérez, B.O.; Pérez, V.M.J. The greener synthesis of nanoparticles. *Trends Biotechnol.* **2013**, *31*, 240–248. [[CrossRef](#)]
113. Ramanathan, A.A.; Aqra, M.W. An Overview of the Green Road to the Synthesis of Nanoparticles. *J. Mater. Sci. Res. Rev.* **2019**, *2*, 1–11.
114. Mahlaule-Glory, L.M.; Mathobela, S.; Hintsho-Mbita, N.C. Biosynthesized Bimetallic (ZnO/SnO<sub>2</sub>) Nanoparticles for Photocatalytic Degradation of Organic Dyes and Pharmaceutical Pollutants. *Catalysts* **2022**, *12*, 334. [[CrossRef](#)]
115. Sorbiun, M.; Shayegan Mehr, E.; Ramazani, A.; Taghavi Fardood, S. Biosynthesis of Ag, ZnO and bimetallic Ag/ZnO alloy nanoparticles by aqueous extract of oak fruit hull (Jaft) and investigation of photocatalytic activity of ZnO and bimetallic Ag/ZnO for degradation of basic violet 3 dye. *J. Mater. Sci. Mater. Electron.* **2018**, *29*, 2806–2814. [[CrossRef](#)]
116. Aldeen, T.S.; Ahmed Mohamed, H.E.; Maaza, M. ZnO nanoparticles prepared via a green synthesis approach: Physical properties, photocatalytic and antibacterial activity. *J. Phys. Chem. Solids* **2022**, *160*, 10313. [[CrossRef](#)]
117. Sedefoglu, N.; Zalaoglu, Y.; Bozok, F. Green synthesized ZnO nanoparticles using *Ganoderma lucidum*: Characterization and In Vitro Nanofertilizer Effects. *J. Alloys Compd.* **2022**, *918*, 165695. [[CrossRef](#)]
118. Zare, M.; Namratha, K.; Thakur, M.S.; Byrappa, K. Biocompatibility assessment and photocatalytic activity of bio-hydrothermal synthesis of ZnO nanoparticles by *Thymus vulgaris* leaf extract. *Mater. Res. Bull.* **2019**, *109*, 49–59. [[CrossRef](#)]
119. Umar, A.; Sabrina, V.; Yulizar, Y. Synthesis of ZnO nanoparticles using *Sapindus rarak* DC fruit pericarp extract for rhodamine B photodegradation. *Inorg. Chem. Commun.* **2022**, *141*, 109593. [[CrossRef](#)]
120. Bopape, D.A.; Motaung, D.E.; Hintsho-Mbita, N.C. Green synthesis of ZnO: Effect of plant concentration on the morphology, optical properties and photodegradation of dyes and antibiotics in wastewater. *Optik* **2022**, *251*, 168459. [[CrossRef](#)]
121. Sangeetha, G.; Rajeshwari, S.; Venckatesh, R. Green synthesis of zinc oxide nanoparticles by aloe barbadensis miller leaf extract: Structure and optical properties. *Mater. Res. Bull.* **2011**, *46*, 2560–2566. [[CrossRef](#)]
122. MalligArjuna Rao, S.; Kotteeswaran, S.; Visagamani, A.M. Green synthesis of zinc oxide nanoparticles from *camellia sinensis*: Organic dye degradation and antibacterial activity. *Inorg. Chem. Commun.* **2021**, *134*, 108956. [[CrossRef](#)]
123. Udayabhanu; Nagaraju, G.; Nagabhushana, H.; Suresh, D.; Anupama, C.; Raghu, G.K.; Sharma, S.C. *Vitis labruska* skin extract assisted green synthesis of ZnO super structures for multifunctional applications. *Ceram. Int.* **2017**, *43*, 11656–11667. [[CrossRef](#)]
124. Tripathi, R.M.; Bhadwal, A.S.; Gupta, R.K.; Singh, P.; Shrivastav, A.; Shrivastav, B.R. ZnO nanoflowers: Novel biogenic synthesis and enhanced photocatalytic activity. *J. Photochem. Photobiol. B Biol.* **2014**, *141*, 288–295. [[CrossRef](#)] [[PubMed](#)]
125. Rashad, M.M.; Ismail, A.A.; Kandil, A.T.; Osama, I.; Ibrahim, I.A. Photocatalytic decomposition of dyes using ZnO doped SnO<sub>2</sub> nanoparticles prepared by solvothermal method. *Arab. J. Chem.* **2014**, *7*, 71–77. [[CrossRef](#)]
126. Chakraborty, S.; Farida, J.J.; Simon, R.; Kasthuri, S.; Mary, N.L. *Averrhoa carrambola* fruit extract assisted green synthesis of zinc nanoparticles for the photodegradation of congo red dye. *Surf. Interfaces* **2020**, *19*, 100488. [[CrossRef](#)]
127. Abdullah, F.H.; Abu Bakar, N.H.H.; Abu Bakar, M. Low temperature biosynthesis of crystalline zinc oxide nanoparticles from *Musa acuminata* peel extract for visible-light degradation of methylene blue. *Optik* **2020**, *206*, 164279. [[CrossRef](#)]
128. Vinayagam, R.; Selvaraj, R.; Arivalagan, P.; Varadavenkatesan, T. Synthesis, characterization and photocatalytic dye degradation capability of *Calliandra haematocephala*-mediated zinc oxide nanoflowers. *J. Photochem. Photobiol. B Biol.* **2020**, *203*, 111760. [[CrossRef](#)]

129. Alshehri, A.A.; Malik, M.A. Biogenic fabrication of ZnO nanoparticles using *Trigonella foenum-graecum* (Fenugreek) for proficient photocatalytic degradation of methylene blue under UV irradiation. *J. Mater. Sci. Mater. Electron.* **2019**, *30*, 16156–16173. [[CrossRef](#)]
130. Hee, K.O.; Rupa, E.J.; Anandapadmanaban, G.; Chokkalingam, M.; Li, J.F.; Markus, J.; Soshnikova, V.; Perez, Z.E.J.; Yang, D.C. Cationic and anionic dye degradation activity of Zinc oxide nanoparticles from *Hippophae rhamnoides* leaves as potential water treatment resource. *Optik* **2019**, *181*, 1091–1098.
131. Madhumitha, G.; Fowsiya, J.; Gupta, N.; Kumar, A.; Singh, M. Green synthesis, characterization and antifungal and photocatalytic activity of *Pithecellobium dulce* peel-mediated ZnO nanoparticles. *J. Phys. Chem. Solids.* **2019**, *127*, 43–51. [[CrossRef](#)]
132. Prasad, A.R.; Garvasis, J.; Oruvil, S.K.; Joseph, A. Bio-inspired green synthesis of zinc oxide nanoparticles using *Abelmoschus esculentus* mucilage and selective degradation of cationic dye pollutants. *J. Phys. Chem. Solids* **2019**, *127*, 265–274. [[CrossRef](#)]
133. Gawade, V.V.; Gavade, N.L.; Shinde, H.M.; Babar, S.B.; Kadam, A.N.; Garadkar, K.M. Green synthesis of ZnO nanoparticles by using *Calotropis procera* leaves for the photodegradation of methyl orange. *J. Mater. Sci. Mater. Electron.* **2017**, *28*, 14033–14039. [[CrossRef](#)]
134. Siripireddy, B.; Mandal, B.K. Facile green synthesis of zinc oxide nanoparticles by *Eucalyptus globulus* and their photocatalytic and antioxidant activity. *Adv. Powder Technol.* **2017**, *28*, 785–797. [[CrossRef](#)]
135. Suresh, D.; Shobharani, R.M.; Nethravathi, P.C.; Pavan Kumar, M.A.; Nagabhushana, H.; Sharma, S.C. *Artocarpus gomezianus* aided green synthesis of ZnO nanoparticles: Luminescence, photocatalytic and antioxidant properties. *Spectrochim. Acta Part. A Mol. Biomol. Spectrosc.* **2015**, *141*, 128–134. [[CrossRef](#)] [[PubMed](#)]
136. Vidya, C.; Manjunatha, C.; Chandraprabha, M.N.; Rajshekar, M.; Antony Raj, M.A.L. Hazard free green synthesis of ZnO nano-photo-catalyst using *Artocarpus Heterophyllus* leaf extract for the degradation of Congo red dye in water treatment applications. *J. Environ. Chem. Eng.* **2017**, *5*, 3172–3180. [[CrossRef](#)]
137. Fu, L.; Fu, Z. *Plectranthus amboinicus* leaf extract-assisted biosynthesis of ZnO nanoparticles and their photocatalytic activity. *Ceram. Int.* **2015**, *41*, 2492–2496. [[CrossRef](#)]
138. Singh, K.; Singh, J.; Rawat, M. Green synthesis of zinc oxide nanoparticles using *Punica Granatum* leaf extract and its application towards photocatalytic degradation of Coomassie brilliant blue R-250 dye. *SN Appl. Sci.* **2019**, *1*, 1–8. [[CrossRef](#)]
139. Rana, N.; Chand, S.; Gathania, A.K. Green synthesis of zinc oxide nano-sized spherical particles using *Terminalia chebula* fruits extract for their photocatalytic applications. *Int. Nano Lett.* **2016**, *6*, 91–98. [[CrossRef](#)]
140. Kumar, C.R.; Betageri, V.S.; Nagaraju, G.; Pujar, G.H.; Onkarappa, H.S.; Latha, M.S. One-pot green synthesis of ZnO-CuO nanocomposite and their enhanced photocatalytic and antibacterial activity. *Adv. Nat. Sci. Nanosci. Nanotechnol.* **2020**, *11*, 015009.
141. Sharma, D.; Kanchi, S.; Bisetty, K. Biogenic synthesis of nanoparticles: A review. *Arab. J. Chem.* **2019**, *12*, 3576–3600. [[CrossRef](#)]
142. Chikkanna, M.M.; Neelagund, S.E.; Rajashekarappa, K.K. Green synthesis of Zinc oxide nanoparticles (ZnO NPs) and their biological activity. *SN Appl. Sci.* **2018**, *1*, 1–10. [[CrossRef](#)]
143. Jayaseelan, C.; Rahuman, A.A.; Kirthi, A.V.; Marimuthu, S.; Santhoshkumar, T.; Bagavan, A.; Gaurav, K.; Karthik, L.; Rao, K.V.B. Novel microbial route to synthesize ZnO nanoparticles using *Aeromonas hydrophila* and their activity against pathogenic bacteria and fungi. *Spectrochim. Acta Part A Mol. Biomol. Spectrosc.* **2012**, *90*, 78–84. [[CrossRef](#)]
144. Kalpana, V.; Kataru, B.A.S.; Sravani, N.; Vigneshwari, T.; Panneerselvam, A.; Rajeswari, V.D. Biosynthesis of zinc oxide nanoparticles using culture filtrates of *Aspergillus niger*: Antimicrobial textiles and dye degradation studies. *OpenNano* **2018**, *3*, 48–55. [[CrossRef](#)]
145. Murali, M.; Mahendra, C.; Nagabhushan; Rajashekar, N.; Sudarshana, M.S.; Raveesha, K.A.; Amruthesh, K.N. Antibacterial and antioxidant properties of biosynthesized zinc oxide nanoparticles from *Ceropegia candelabrum* L.—An endemic species. *Spectrochim. Acta Part A Mol. Biomol. Spectrosc.* **2017**, *179*, 104–109. [[CrossRef](#)] [[PubMed](#)]
146. Ali, K.; Dwivedi, S.; Azam, A.; Saquib, Q.; Al-Said, M.S.; Alkhedhairi, A.A.; Musarrat, J. Aloe vera extract functionalized zinc oxide nanoparticles as nanoantibiotics against multi-drug resistant clinical bacterial isolates. *J. Colloid Interface Sci.* **2016**, *472*, 145–156. [[CrossRef](#)] [[PubMed](#)]
147. Santhoshkumar, J.; Kumar, S.V.; Rajeshkumar, S. Synthesis of zinc oxide nanoparticles using plant leaf extract against urinary tract infection pathogen. *Resour. Technol.* **2017**, *3*, 459–465. [[CrossRef](#)]
148. Awwad, A.M.; Amer, M.W.; Salem, N.M.; Abdeen, A.O. Green synthesis of zinc oxide nanoparticles (ZnO-NPs) using *Ailanthus altissima* fruit extracts and antibacterial activity. *Chem. Int.* **2020**, *6*, 151–159.